OCEAN WATER COLOR ASSESSMENT FROM ERTS-1 RBV AND MSS IMAGERY

Donald S. Ross
INTERNATIONAL IMAGING SYSTEMS
510 Logue Avenue
Mountain View, California 94043

October 1973
Final Report for Period September 1972 to October 1973
TR-C200-4

Prepared for
GODDARD SPACE FLIGHT CENTER
Greenbelt, Maryland 20771

TECHNICAL REPORT STANDARD TITLE PAGE

1. Report No.	2. Government Accession No.	3. Recipient's Catalog No.

4. Title and Subtitle	5. Report Date
OCEAN WATER COLOR ASSESSMENT FROM ERTS-1 RBV & MSS IMAGERY	24 Oct. 73
	6. Performing Organization Code
7. Author(s)	8. Performing Organization Report No.
D. S. Ross	TR-C200-4
9. Performing Organization Name and Address	10. Work Unit No.
INTERNATIONAL IMAGING SYSTEMS 510 Logue Avenue Mountain View, California 94043	11. Contract or Grant No. NAS5-21862
	13. Type of Report and Period Covered III- 7 Sep. 72 - 24 Oct. 73
12. Sponsoring Agency Name and Address	14. Sponsoring Agency Code
GODDARD SPACE FLIGHT CENTER Greenbelt, Maryland 20771 E. W. Crump, Technical Monitor	

15. Supplementary Notes

16. Abstract

Experimental objective was to isolate in ERTS-1 coverage of the Bahamas-Caribbean region, image densities of deep ocean water in a 465-490 nm spectral region included in RBV-1 but not found in the similar MSS-4 record; thus dividing the RBV-1 image into "blue" and green records for water color estimation. Photographic interactive image masking was employed, and was also used for reducing residual RBV shading errors. The RBV-2 image was used to cancel shallow water image densities in a 580-600 nm region of MSS-4 before its use as a mask with RBV-1. Variations in haze effects between spectral bands were found by graphical solution based on density differences between cloud and water surface, from which factors for correcting haze effects were determined. The blue and green records produced by masking satisfied the purpose for qualitative analysis. The masking technique can be made simple and rapid, and has many other earth resources applications.

17. Key Words (Selected by Author(s))	18. Distribution Statement
Ocean Color, Interactive Image Processing; Atmospheric Effects; Correcting RBV Shading Errors.	Original photography may be purchased from: EROS Data Center 10th and Dakota Avenue Sioux Falls, SD 57198

19. Security Classif. (of this report)	20. Security Classif. (of this page)	21. No. of Pages	22. Price*
Unclassified	U		

*For sale by the Clearinghouse for Federal Scientific and Technical Information, Springfield, Virginia 22151.

TABLE OF CONTENTS

LIST OF ILLUSTRATIONS

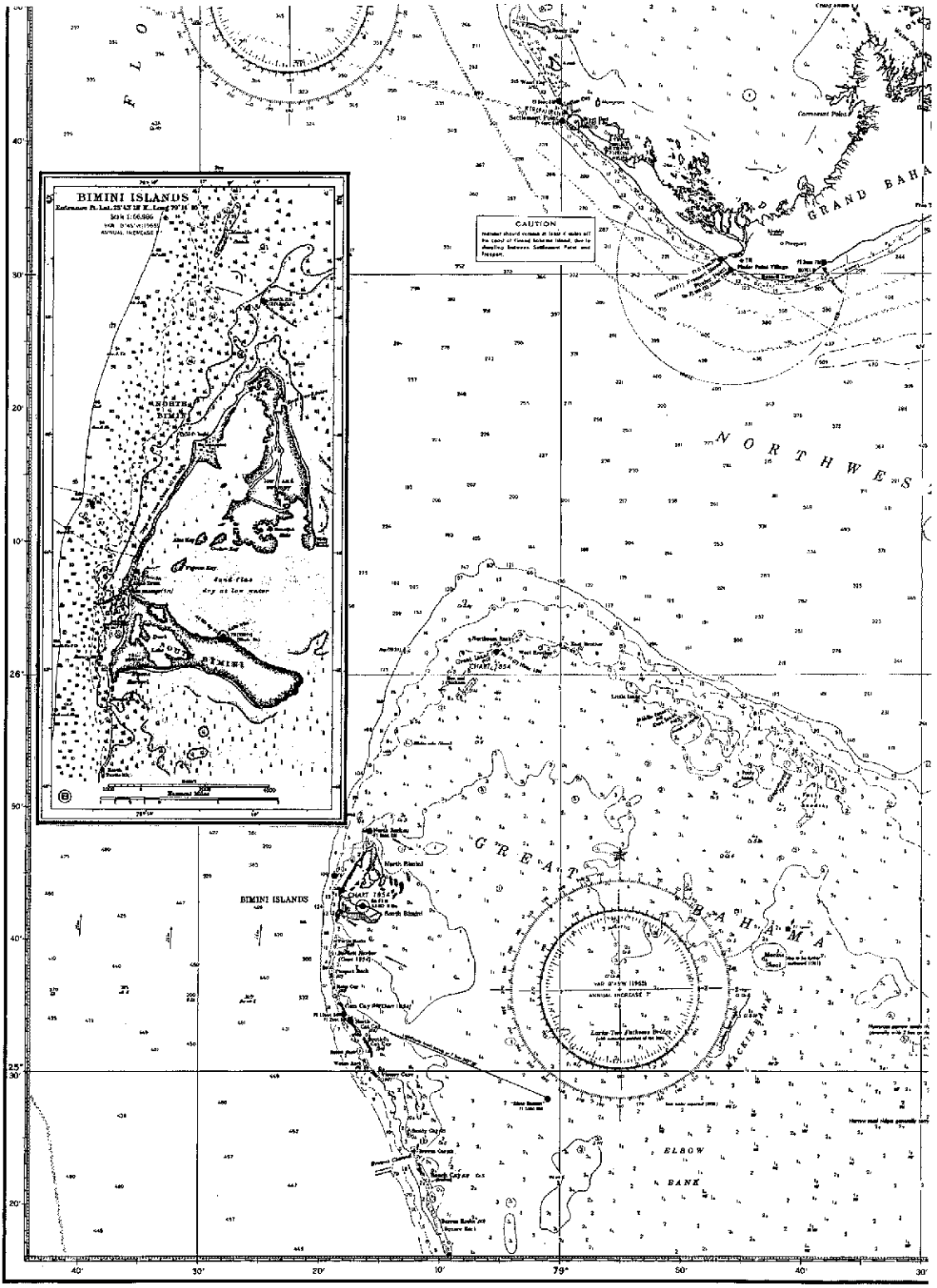

FRONTISPIECE
CHARTS OF BIMINI ISLANDS AND BAHAMAS REGION

PREFACE

The objective of isolating a very narrow region from a broad spectral band in an ERTS-1 image appears to have been met qualitatively in this experiment, but one example is insufficient to prove that repeatible results can be obtained. However, whether or not masking techniques are successful in solving this specific problem is not as important as recognizing the power and utility of these methods for the interactive processing of aerospace multispectral imagery in many other applications. Masking provides a rapid, economical means of performing complex image data reduction tasks which otherwise can only be handled in a computer; as such, it can serve as an editing tool for selecting images which warrant the time and expense of computer processing.

The image masking processes discussed in this report are inherently simple, but do not lend themselves to brief explanation. For a more concise narrative, many details on equipment, image data and procedures are placed in Appendices.

The invaluable assistance of Paul Fedelchak of International Imaging Systems is acknowledged, in carrying out the masking operations described.

OCEAN WATER COLOR ASSESSMENT FROM ERTS-1 RBV AND MSS IMAGERY

1.0 INTRODUCTION

1.1 Brief History of the Project. The Earth Resources Technology Satellite-1 (ERTS-1) acquires images in two spectral regions where it appeared possible that blue and green ocean water color ratios, significant to oceanographers, might be determined by simple photographic masking processes. The Return Beam Vidicon-1 sensor (RBV-1) responds in the 465-580 nm band, while the Multispectral Scanner-4 (MSS-4) records in a 490-600 nm region. The aim of the investigation was to isolate photographic image densities, representing the difference in spectral response between the two; in the 465-490 nm as a blue band, for comparison with a 490-580 nm green record which would also result from the masking techniques.

1.2 Contact was made with other ERTS Principle Investigators, whose projects involved measurement of ocean water color at their test sites at time of ERTS-1 overpass. This would provide ground truth. A primary site in Monterey Bay, California was selected, and the cooperation of the PI, Dr. Richard Miller of Oceanographic Services was freely offered. Unfortunately the ERTS-1 RBV sensors, critical to the plan, were turned off for technical reasons on 6 Aug. 1972 after only 13 days of operation. None of the RBV images acquired, for weather or other reasons, coincided with collection of spectral measurements at any of the primary or secondary test sites.

1.3 After review of available RBV imagery, an alternate area of investigation in the Caribbean was chosen and approved for the experiment. This included Grand Bahama Island, North and South Bimini Islands and the Grand Bahama Bank, as well as large areas of very deep ocean. The characteristics of

water color in this region, and spectral information on upwelling light in the shallows were well-established from previous work by many investigators, including this PI. Duplicate 240 mm (9.5-inch) RC-8 natural color imagery was also available for reference to green and blue water areas; this was taken by NASA/MSC on Mission 147 in 1971 of typical deep and shallow waters in this vicinity, at a scale of 1:120,000 through most of the atmosphere.

1.4 In the absence of direct ground truth measurements it would not be possible to test the data reduction method quantitatively, but at least qualitative assessment of relative blue/green water color ratios might be possible.

1.5 Examination of a series of bulk-processed 240 mm (9.5-inch) positive input RBV transparencies taken on different days showed there were persistent, stationary residual radiometric correction errors, appearing as marked density variations, unique to each band. These were also found in the precision-processed imagery. Photographic masks were made to reduce the stationary density variations in the bulk-processed images as much as possible.

1.6 It was anticipated that density information of the ocean surface images would be biased by atmospheric effects, and a procedure was worked out for estimating these, and adjusting gammas between the working images to the same relative scale.

1.7 The final images have large differences in density in the deep water region, attributable to differences in the blue and green ratios of water color. Visually, the two images appear as expected, conforming with theory.

2.0 TECHNICAL BACKGROUND

2.1 Significance of Ocean Water Color. The color of ocean water is an indicator of many properties and characteristics of the water itself, and indirectly may provide evidence of external dynamic processes which influence its apparent color. If deep ocean water is green, rather than blue, this may be evidence of upwelling nutrients from the depths in sufficient concentrations to support commercially attractive fish populations. Similarly a shift from the blue to green may outline the boundaries of two water masses; or show the configuration and direction of flowing currents. In some circumstances rates of flow may be calculated. The detection of effluents and pollutants in offshore waters and in estuaries is aided by water color determination, and direct identification of the nature of the substances may be possible. Shoreline erosional processes and their extent and rate may be estimated by knowledge of how sediment loads change the spectral appearance of the water. Estimation of water depth and insight into bottom composition are also applications where water color can be significant to the investigator.

Interpreting and identifying causes of water color, and the application of this information to useful purposes are matters for physical, hydrological, and biochemical oceanographic specialists. First, however, it is necessary to provide spectral and spatial image data on the color and distribution of the waters concerned.

Potentially, ERTS (and future similar satellites) make it possible to collect contiguous water color information over vast ocean and coastal areas in a volume and tempo never before possible. Previously, similar data could only be collected at any one time from a limited number of positions, dispersed over the wide areas now recorded by the satellite in a matter of minutes.

2.2 ERTS Sensor Spectral Response and Water Color. Major information on ocean water characteristics is deduced from its green and blue color ratios. Visually, blue is 470 to 480 nm; at 460 nm a sensation of blue-violet occurs, and between 480-490 nm a blue-green, or cyan hue is seen.

A chlorophyll absorption peak occurs in the 430 nm region, and is of interest for aiding the detection of phytoplankton in the sea. Figure 2-1 illustrates the spectral distribution of upwelling light in very clear, deep ocean water.(1) The peak occurs between 460 and 490 nm. As longer wavelengths are approached, absorption becomes almost complete above 700 nm, in the near infrared region.

In clear, shallow water, light reflected from light-colored bottom may be found in the green, and to some degree in the red region according to water depth, as shown in the spectroradiometric plot in Figure 2-2.(1) White, calcareous sand, common in the Bahamas area, has spectral reflectance characteristics of the kind shown in Figure 2-3,(1) where beaches and shoals are exposed or covered with a half-meter of water, or less. Whether deep or shallow, water containing suspended particles of biological origin or certain inert materials takes on a green, greenish-yellow (or even red) appearance according to the size, composition, mixture and concentration of particulates. As penetration of light into the water is diminished, by suspended material and solutes, predominant wavelengths shift toward the green and red region. Red tide is primarily a surface effect, as far as remote sensing is concerned.

The passband limits of ERTS-1 spectral response for RBV-1, RBV-2 and MSS-4 are shown relative to the upwelling light in Figures 2-1 through 2-3; this relationship is significant for an understanding of how the deep and shallow water will be recorded in each ERTS band, and how the masking processed will operate.

Figure 2-4 shows the relative response envelopes of ERTS-1 bands 1 and 2, which have 10% or more response respectively in the 465-580 nm and 580-680 nm spectral regions; also the MSS band 4, calculated to span the 490-600 nm region. RBV-1 thus has significant response in a narrow band between 465 nm and 490 nm, a spectral region not included with the response of MSS-4. The 465-490 nm band is associated with the distinctive blue color of upwelling light in clear, calm, deep ocean water; water barren in the biological sense, and free of inert materials in suspension.

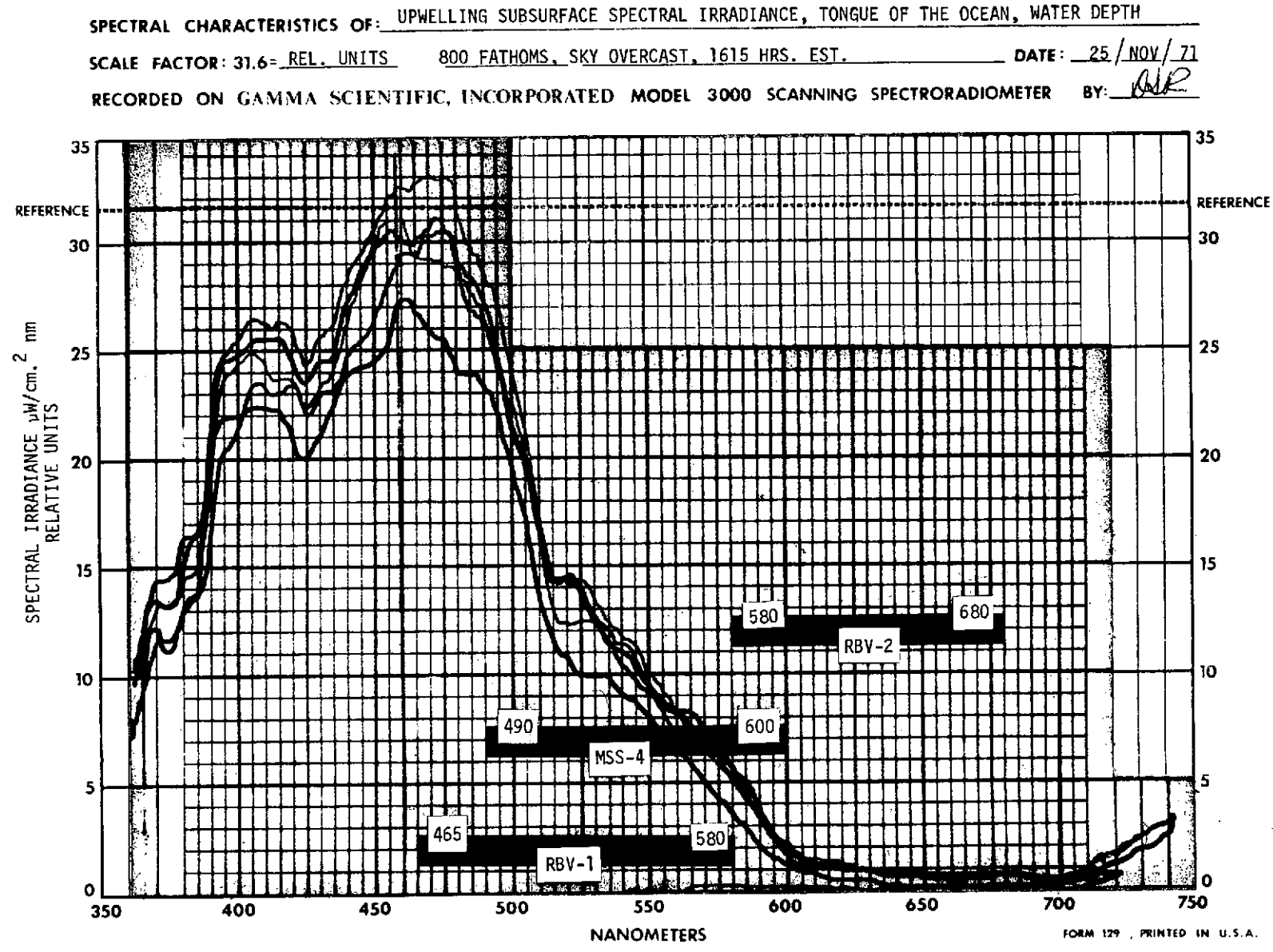

Figure 2-1 Spectral recording of light from deep water,[1] and ERTS-1 band limits for RBV-1, RBV-2 and MSS-4.

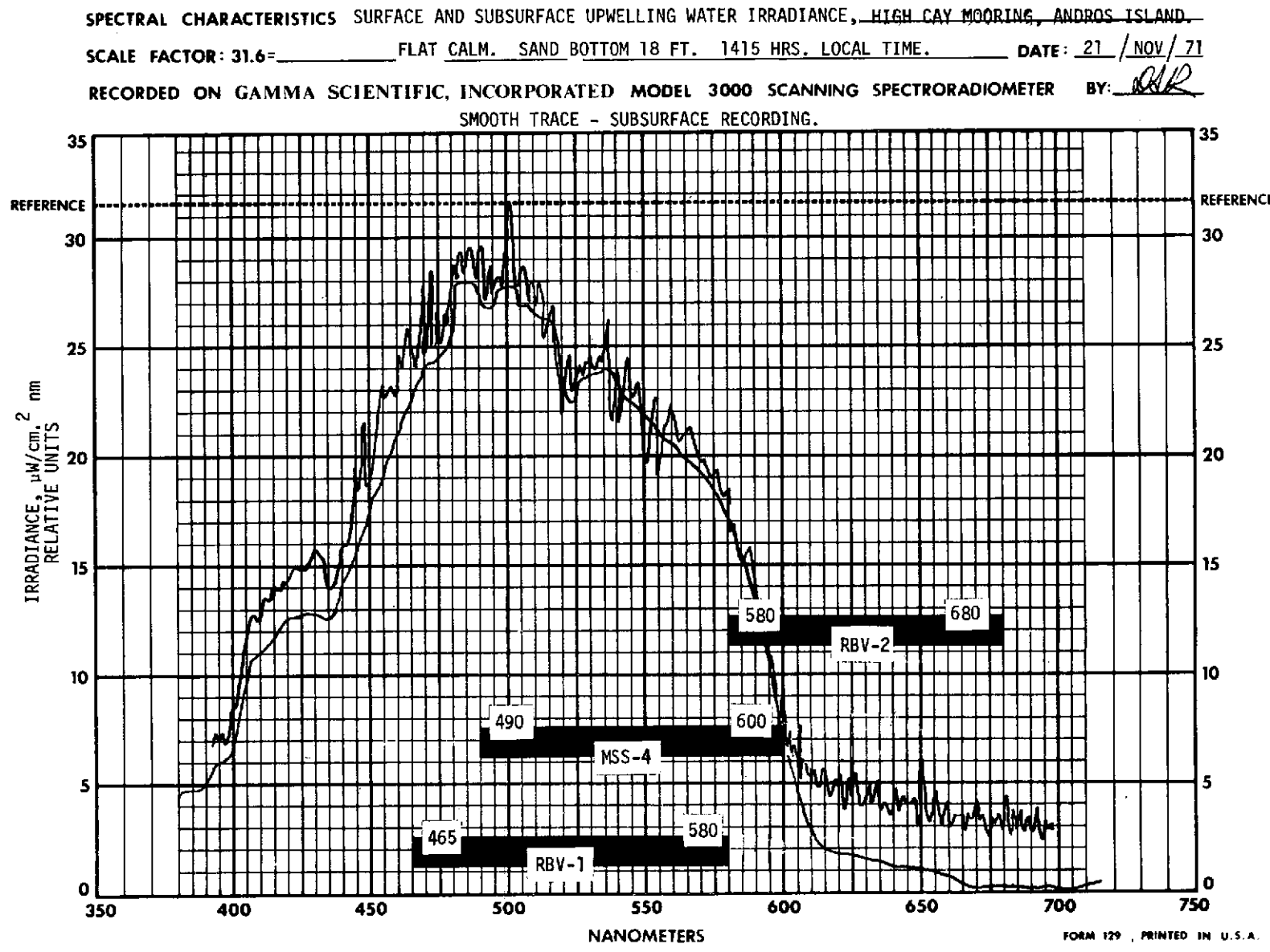

Figure 2-2 Surface and subsurface upwelling light in water 5.5 meters deep, white sand bottom,[1] with spectral band limits for ERTS-1 RBV-1, RBV-2 and MSS-4.

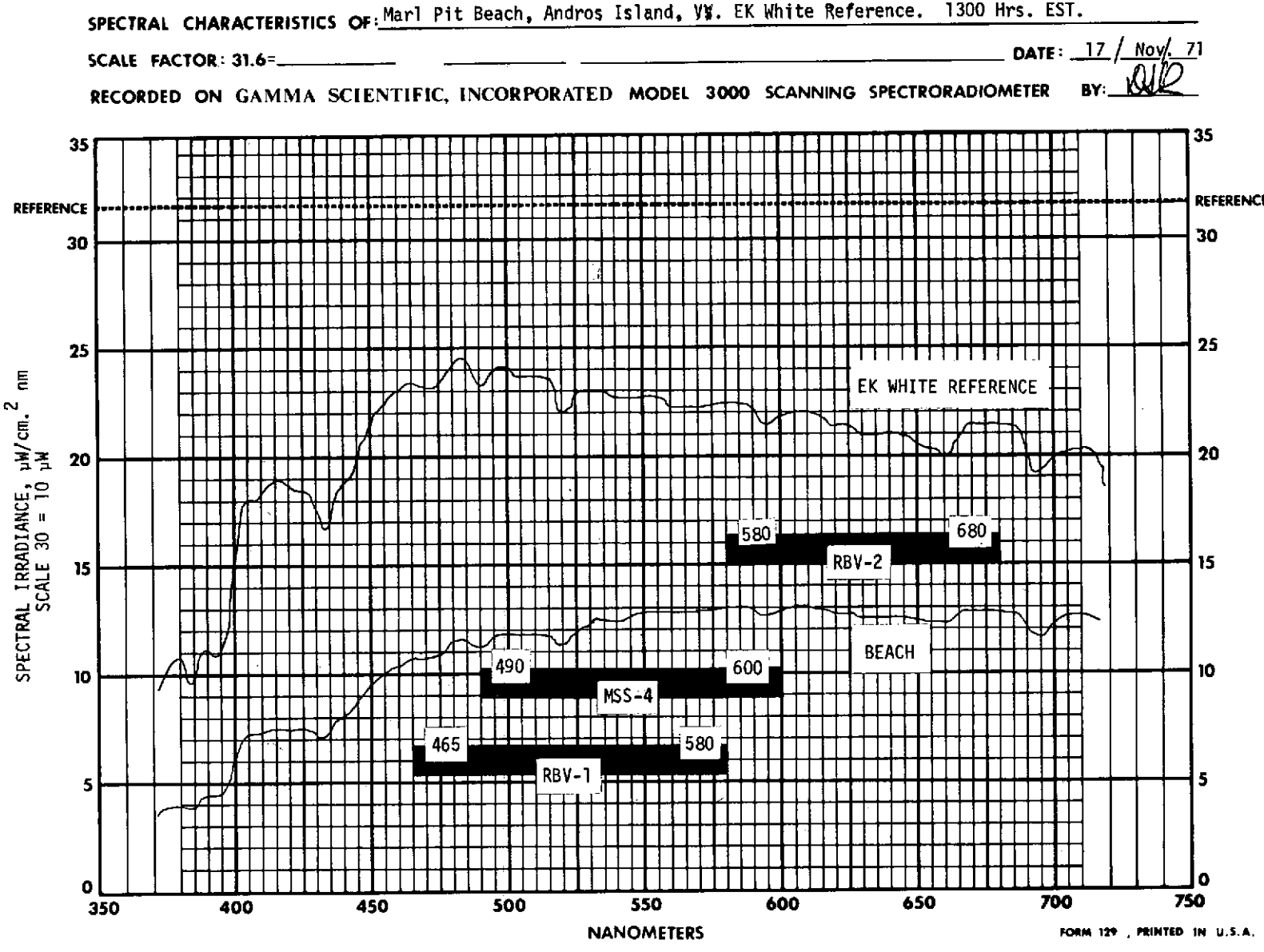

Figure 2-3 Spectral recording of light from typical Bahamian beach, compared with spectral white reference,[1] and ERTS-1 RBV-1, RBV-2 and MSS-4 band limits.

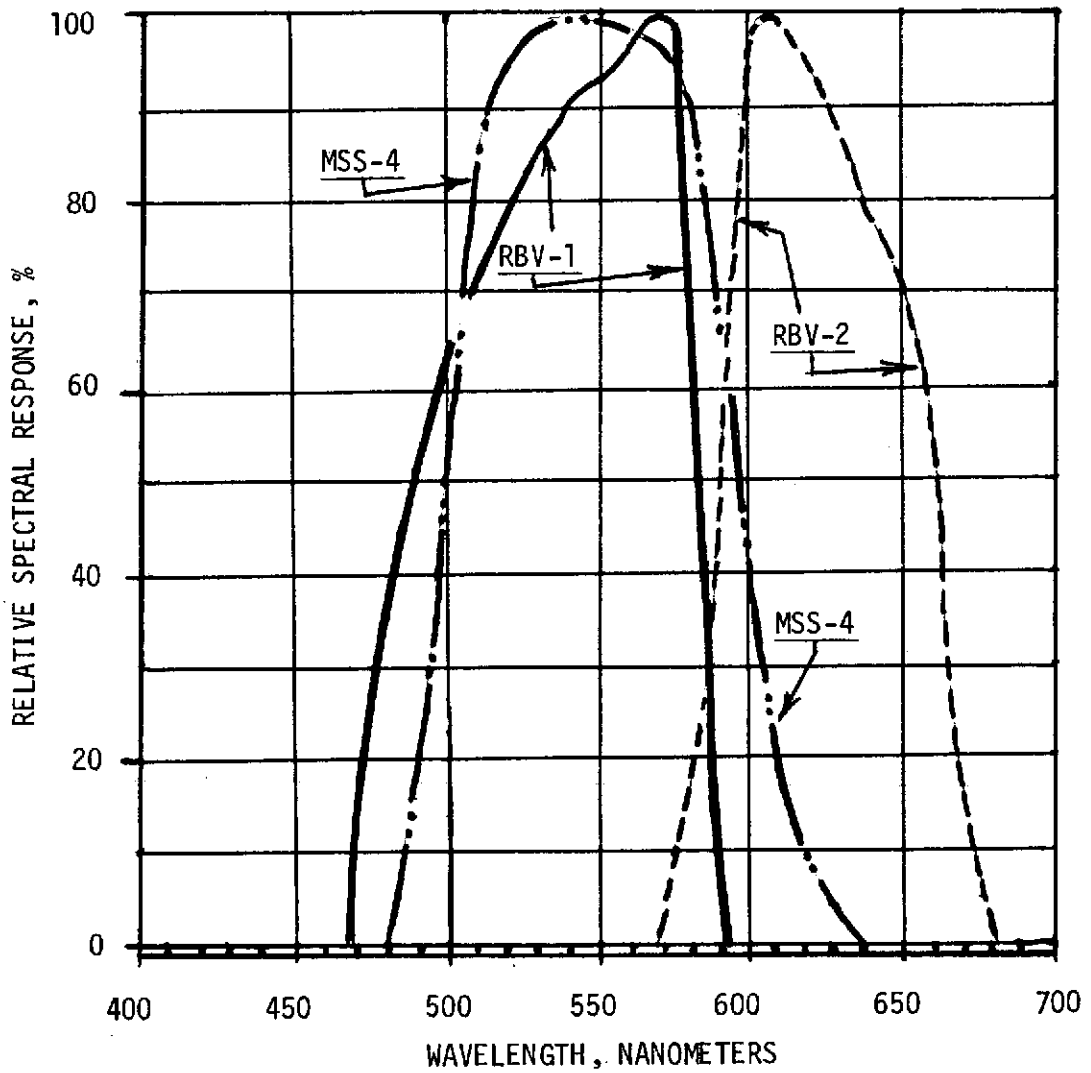

Figure 2-4 Spectral envelopes of ERTS-1 RBV-1, RBV-2 and MSS-4 response bands, derived from Reference (2).

The present ERTS sensors do not include a spectral band specifically dedicated to the blue spectral region, and the only opportunity to determine the significant blue/green water color ratios depends on using the spectral differences recorded between the two "green" bands; the RBV-1 and MSS-4 records.

2.3 Photographic Masking. In normal photographic masking, a negative is registered image-wise with a positive transparency (mask) which has been made from it. By controlling the density and/or contrast of the mask, the densities and/or contrast of a new image printed from the composite may be modified selectively. Masking is widely used in printing color transparencies in graphic arts processes for altering the characteristics of the input to match the hue and chroma characteristics of the color reproduction materials or printing inks.

In multispectral interactive image processing, the density and contrast of a masking image made from one spectral record can be produced at density/contrast values which modulate the density/contrast values of a different spectral record in a predetermined manner, such as the cancellation or modification of spectral reflectances which are at common levels in each record.

In isolating the spectral differences between the 465-580 nm record obtained with RBV-1 and the MSS-4 490-600 nm record, interactive image processing by photographic masking offers a relatively rapid and economical technique, which requires only a modest outlay in equipment which can be found in many photographic laboratories capable of controlling standard sensitometric procedures.

As the ERTS-1 input photographic images are essentially analog representations of the digital tape records of sensor response, masking with photographic materials may be visualized as a means of analog data processing. The fact that the whole image may be treated simultaneously, rather than by pixel by pixel and line by line, with simple processes and equipment, underlines the advantages in speed and economy to be gained by this technique. At the least, such methods can be carried out by

technicians to give a rapid evaluation of whether or not it is worthwhile to expend the efforts of a discipline scientist and the expensive computer time required for a detailed digital analysis of the image.

Figure 2-5 illustrates how image reflectances common to two different spectral bands may be cancelled by photographic masking. In this set of images, the water surface and its image of reflected sun and skylight, swells and a few whitecaps are common to both images, whereas the distribution and concentration of the rhodamine dye occurs only in one image. Masking is done by generating one image as a positive and the other as a negative, where the relative densities and gammas (or contrast) between the two are carefully matched. When the two images in opposite polarity are registered image-wise, densities of image detail common to both are cancelled or "masked". A third photographic print made from this combination thus contains only densities in image information which are different between the two spectral bands, and all redundant information is removed.

2.4 Water Image Densities vis-a-vis Spectral Bands. In the example of masking shown in Figure 2-5 the dye appears in only one of the two spectral bands, and its isolation is almost complete in the masked image. In applying the technique to ERTS images, however, the spectral characteristics of upwelling light in the water are not as sharply defined, particularly in shallow water, as can be seen from Figures 2-1 and 2-2.

In images of the deep water, which is predominently blue, densities should represent primarily only spectral radiances below 500 nm in the RBV-1 image; consequently, in the MSS-4 image, the same ocean areas should have less density in the negative (a higher density in the positive) since MSS-4 has no response below 490 nm.

In the shallow water where upwelling light includes a strong component from bottom reflection, the RBV-1 and MSS-4 bands will both record the green and yellow region, from 500 nm to about 600 nm.

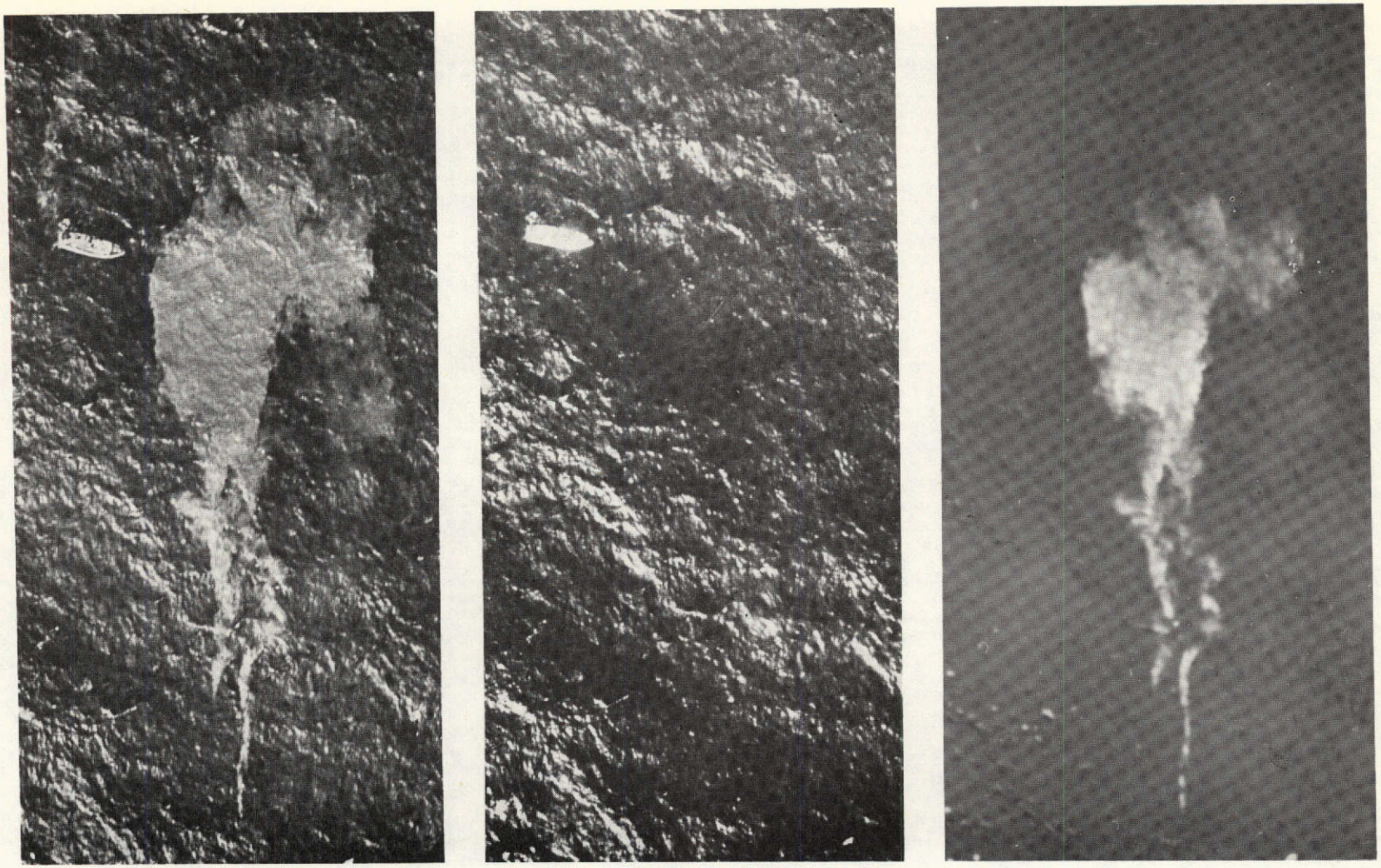

A. Rhodamine dye on sea, 615 nm.

B. Simultaneous photograph, 760 nm.

C. Product of A neg minus B pos.

Figure 2-5 Masking with multispectral images to remove spectral scene reflectances of similar values.

RBV-2, nominally a red band, has about 20% sensor response at 580 nm (yellow). It should not record the deep ocean surface, but it will record some upwelling light in the shallow areas from reflective bottom.

2.5 Water Surface Effects. The calm water surface reflects less than 5% of incident skylight in the 400-700 nm region with sun elevation above 30°.(3) Waves and whitecaps will reflect much more, and at ERTS image scales and resolution may become integrated as areas of higher surface reflectance with a form which can be mistaken for suspended sediment. If such areas appear in all spectral bands at about the same density level, particularly in the infrared ERTS bands, the effect is likely to be caused by whitecaps rather than sediment.

2.6 Photographic System Densitometry. For accurate masking and image reproduction, knowledge of input image sensitometric factors and sensitometric control of all subsequent steps is required. The density and gamma ranges of NASA/GSFC input images are specified and adhered to within close tolerances, thus providing basic information on the relationship of image scene densities as they are recorded through the atmosphere in the different spectral bands. Calibrated step wedges and densitometry are adequate for the further control necessary for reproduction in the masking processes.

2.7 Atmospheric Effects. Rayleigh and Mie scattering of light into an atmospheric haze imposes a serious, and usually unknown variable on the spectral characteristics of the scene, by distorting and degrading scene albedo values. This effect is greatest in the ERTS-1 RBV-1 and MSS-4 green sensor regions, and requires correction; at least to the point where scene contrast values can be made relative between the spectral bands to be used in masking.

2.8 Additional ERTS-1 Image Corrections. For the experiment it would be necessary to consider two additional factors which influence image density and contrast. These were stationary residual radiometric correction errors which appeared evident in the RBV images used for the project; and the decrease in image contrast caused by fall-off in

sensor output at response levels of less than 20% of full scale,[2a] an effect which lowers the contrast in dark parts of the scene in all bands, where the ocean may be recorded in the positive image.

3.0 TECHNICAL PROCEDURE

3.1 Masking Scheme. Figure 3-1 illustrates the masking scheme adopted for producing from the RBV-1 image two new images: X representing a 465-490 nm record and Y, a 490-580 nm record; the blue and green water color components respectively. Essentially this would be done by masking an RBV-2 positive (B) with an MSS-4 negative (C). The positive product (D) would now represent water image densities in the 490-580 nm region, a 580-600 nm yellow band common to both input images having been removed by masking; and consequently removed from upwelling light in the shallows and sandy areas (Figures 2-2, 2-3). Removal of this band should have little or no effect on the deep water image, since the water is blue, not yellow.

The polarity of (D) is made negative in (E) and registered with the 465-580 nm RBV-1 positive (G). The product of this composite negative, X (or H) will be a record of image densities in RBV-1 of the 465-490 nm blue region, (E) having cancelled other densities attributable to the 490-580 nm region common to (E) and (G). The cancellation of this band will substantially reduce image densities in the shallow and sandy areas as shown in Figures 2-2 and 2-3; but to a much lesser extent, those in the deep water areas, Figure 2-1.

The 465-490 nm negative X (or H) would then be registered with RBV-1 positive (G) to produce the negative Y (or I), having densities in the ocean scene representing the 490-580 nm spectral region. Negatives X and Y would then represent the blue and green upwelling light in the water, with image densities which could be equated for water color assessment.

3.2 The set of images selected for the work was 1007-15165, further details on which are given in Appendix A. Figures 3-2 through 3-4 are reproductions of the RBV-1, -2 and MSS-4 spectral bands. Image density measurement reference areas used for sensitometric control are marked in Figure 3-2. A hydrographic chart of the general region appears as the frontispiece of this report.

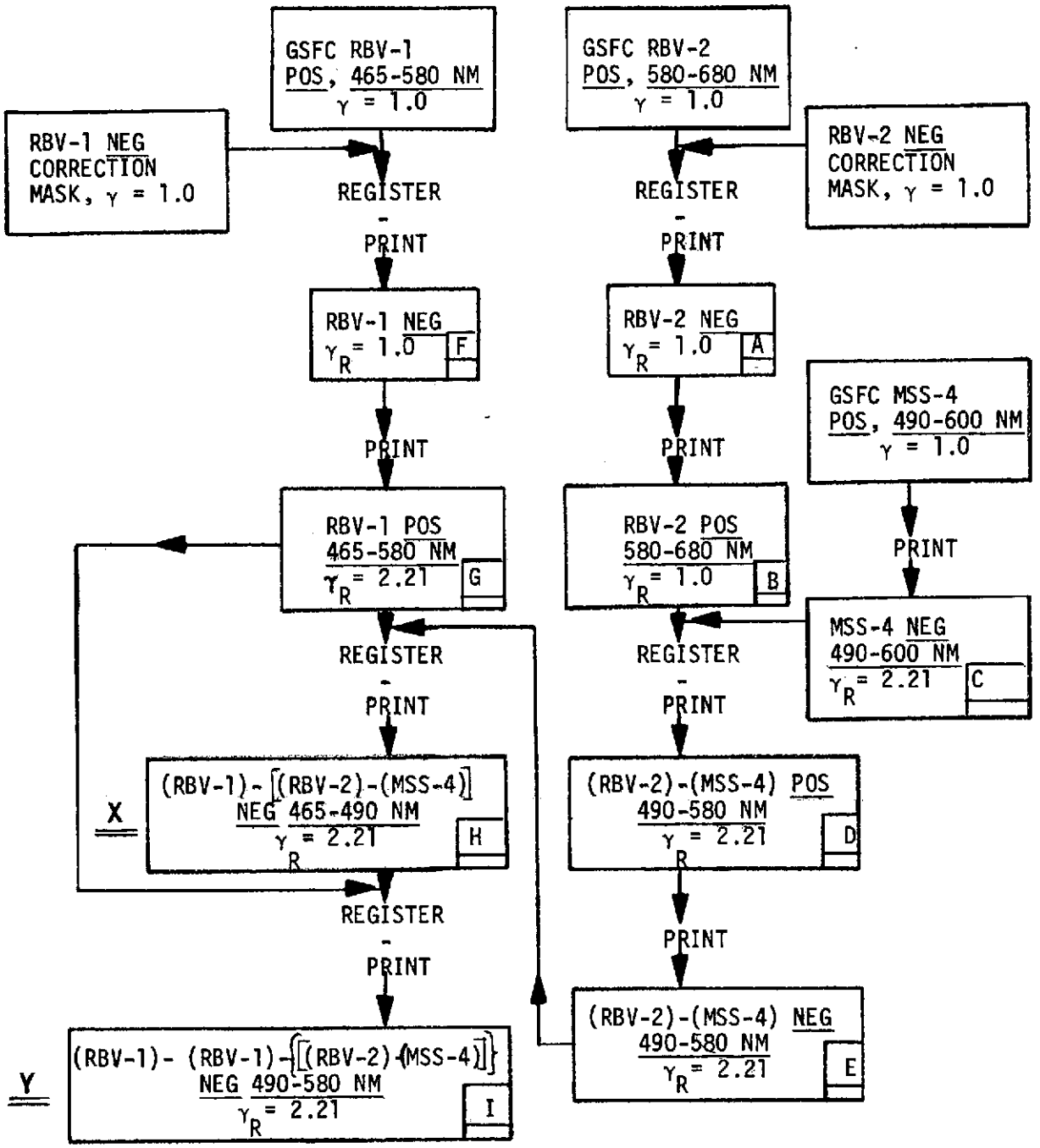

Figure 3-1 Masking steps for producing negatives X and Y. The scene reproduction gamma (γ_R) is shown for each stage. The letters in the blocks identify control step tablet printing positions.

Figure 3-2 ERTS-1 1007-15165-1. RBV-1 image of Bahamas region. The image has been masked for correcting residual shading errors. (See Para 3.4.) The dark clouds on the left are from clouds in the correction mask image. Some image areas used for reference density measurements are identified.

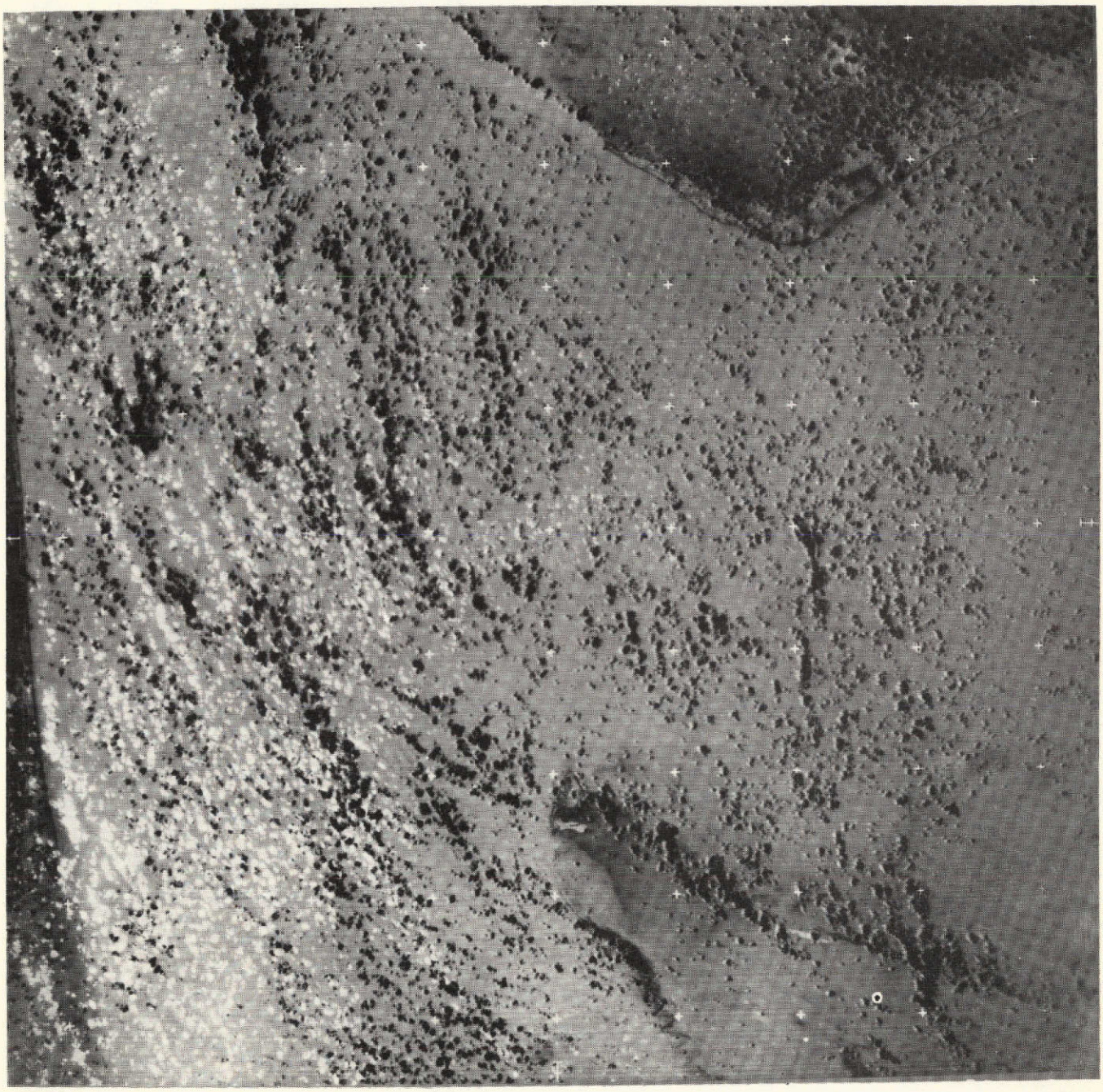

Figure 3-3 ERTS-1 1007-15165-2. RBV-2 image of Bahamas region. This image is reproduced as a negative to retain detail in the ocean area for the half-tone printing process. Clouds in the correction mask appear white.

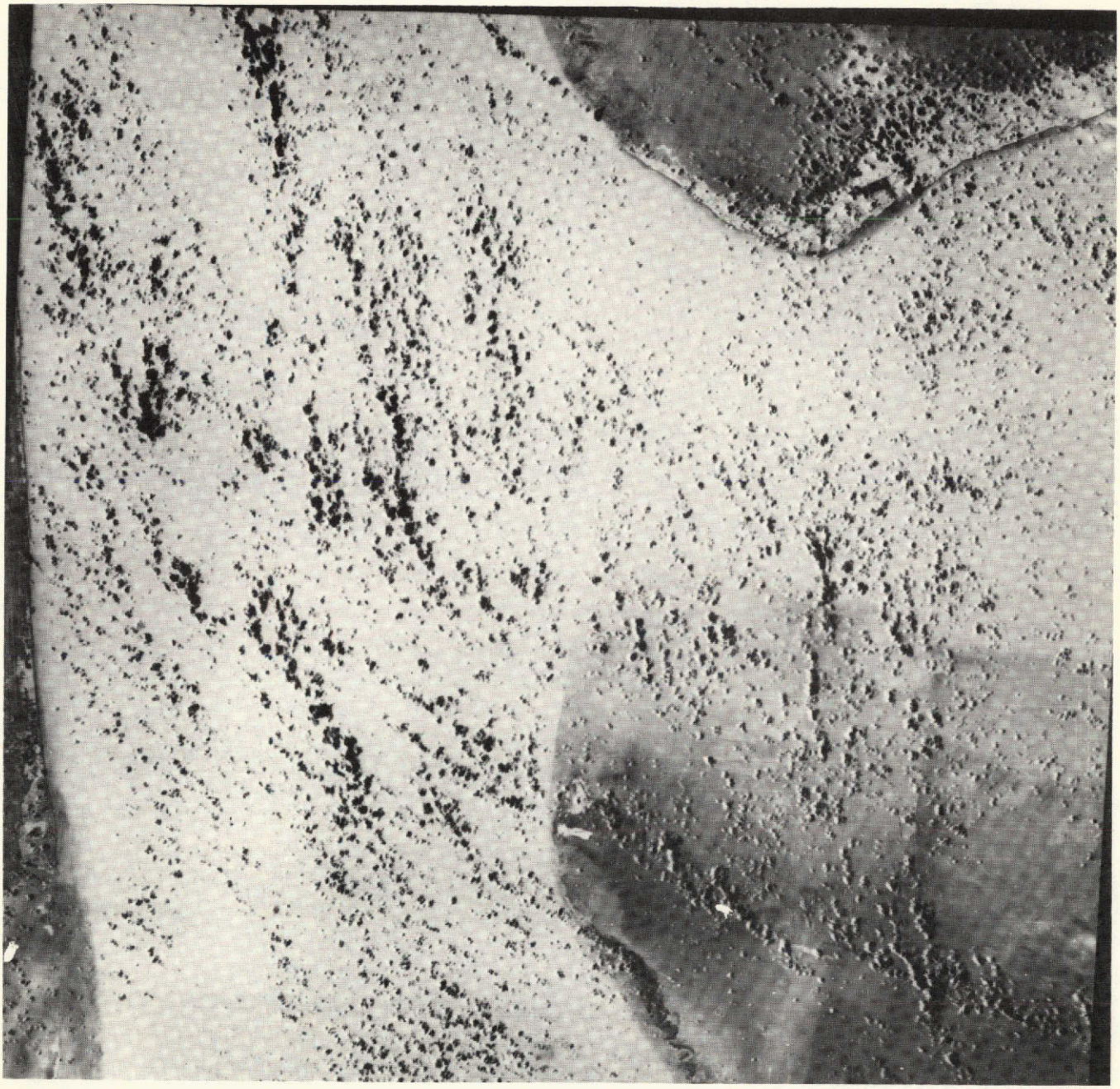

Figure 3-4 ERTS-1 1007-15165-4. MSS-4 image of Bahamas region. Reproduced as a negative to retain water detail for half-tone printing.

3.3 As recorded scene contrast was different between the RBV-1/MSS-4 image pair, and the RBV-2 image because of atmospheric haze effects in the two spectral regions, it was found necessary to estimate the order of difference and make corrections as described below. First, however, masking was used to correct residual shading in the RBV images.

3.4 RBV Image Correction for Recording Stationary Residual Radiometric Errors.* The non-uniform radiance-response on the surface of the individual RBV tubes was calibrated by NASA/GSFC, and the calibration data were used to generate a response-smoothing program in an 18 X 18 matrix for post-acquisition image signal processing.[2b] A review of numbers of RBV images showed, however, that visible, local density variations occurred in the same position in each of different image-scenes taken in the same band, on different days. RBV-1, -2 and -3 images were individually so affected.

To correct these repetitive local density variations, photographic masks of opposite density polarity were made for the RBV-1 and -2 images, to produce new working negatives, identified in Figure 3-1 as RBV-1 (F) and RBV-2 (A).

The masks were made from bulk-processed 240 mm (9.5 inch) RBV-1 and -2 images of a relatively cloud-free ocean area (E-1007-15160-1 and -2) by contact printing, and processing to γ1.0. Exposure was adjusted by trial and error until the combination of the processed negative mask, registered with the original positive RBV-1 image in the set, showed by measurement that density variation on the ocean surface was in the order of density variations found in the MSS-4 image of the same scene, which was free of the type of error being corrected. The RBV-1 scene before and after masking is reproduced in Figure 3-5.

The ERTS images are reproduced at γ1.0, but the dark parts of the scene, because of sensor response, decline from this value.[2a] The mask was made on Kodak Commercial film (4127) developed in D-19, and the toe of

* Reported in more detail in "Experimental Masking of RBV Images to Reduce Stationary Residual Inaccuracies in Radiometric Correction", Symposium on Significant Results Obtained from the Earth Resources Technology Satellite-1, Vol. 1, Sect. B, pp. 1123-1128.

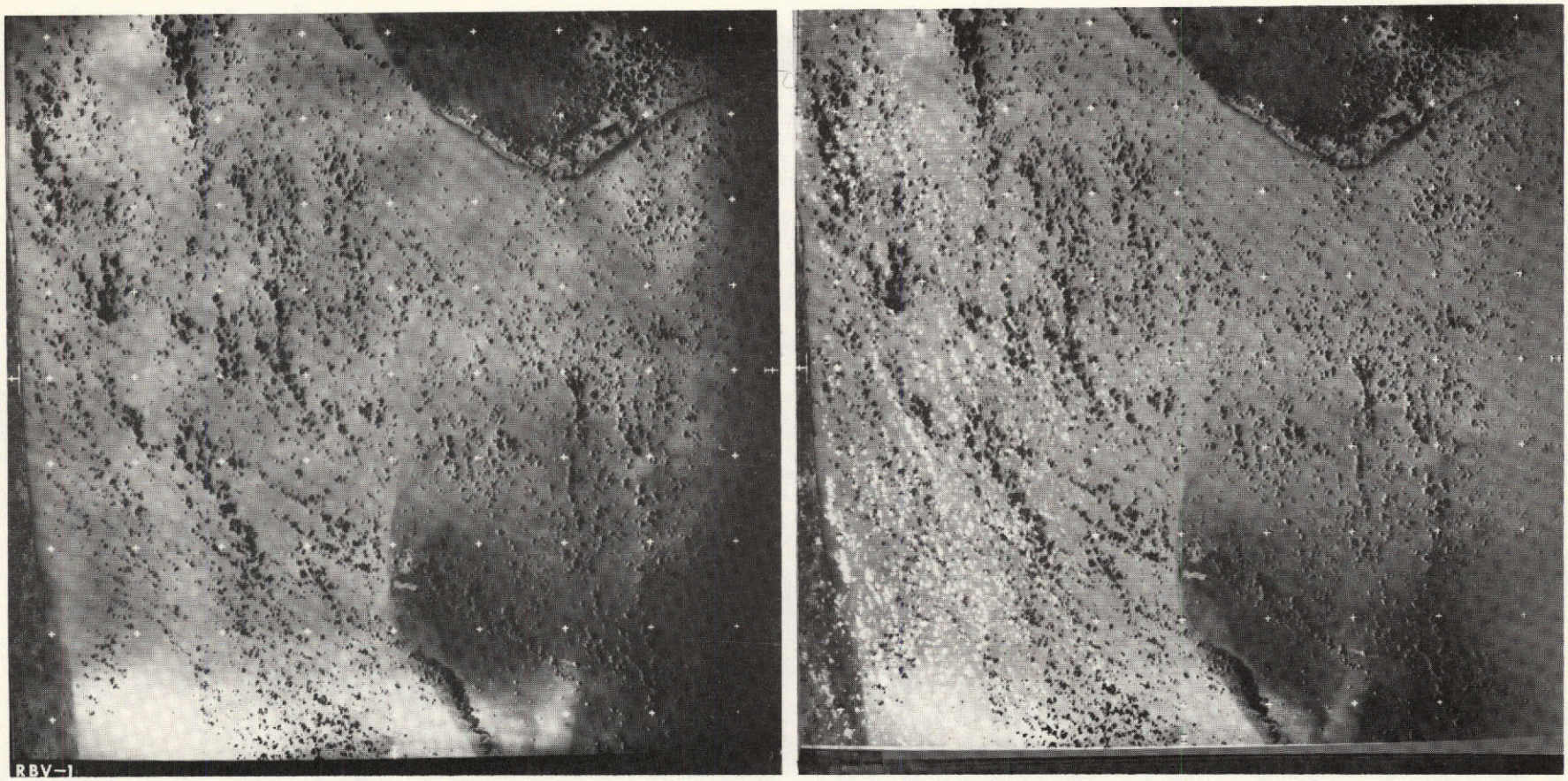

Figure 3-5 Left, RBV-1 image before masking showing repetitive residual shading errors. Right, RBV-1 image reprinted with correction mask.

the response curve for this film exhibits a similar departure from γ1.0, providing an almost perfect match in density/gamma cancellation.

In an unmasked RBV image, local density variations as large as 0.60 were found, compared with the same areas in the MSS image, a 4:1 transmittance difference. This was reduced to $\pm$0.03 D, in the same areas in the composite mask plus original; or $\pm$1.35 T. Such masks, made at γ1.0 can be used with any RBV images made in the same spectral band to reduce residual correction errors, but density levels may have to be adjusted to match density variations permitted in the specification for the images being masked. The NASA/GSFC tolerance is $\pm$0.12 D in the 0.40 - 2.40 D range of the reproduced images, and gamma is 1.0 $\pm$0.1.[2a] The highest mask densities average 0.50, and fall on a part of the reproduction curve where average gamma is about 0.60, the gamma tolerance would be about $\pm$0.06. Density-wise, this would be $\pm$0.03 relative to the average density of 0.50 (D0.50 X γ0.06). This is in the order of local variation in development and combined errors in densitometry, and for the purposes of this technique can be ignored in view of the large practical gains made in all-over radiometric error smoothing.

3.5 Estimating Contrast Degradation by Haze and Sensor Response. These corrections are interrelated and will be treated together. The effect of atmospheric haze (path radiance, or air luminance) is to compress the contrast of the lower scene radiances, or reflectances more than the higher, in a non-linear fashion. Sets of curves have been developed showing the effect of various percentages of haze on image illumination received by a sensor,[4] and for relating haze effects to normalized film densities, or scene radiance/reflectance values.[5] The curve shown in Figure 3-6 provides a graphic way of estimating the order of haze effects in degrading scene contrast under average atmospheric conditions, if the percentage of haze is known. Brock[6] notes that transmission in the atmospheric and haze effects can be found by measuring the image densities (at known gamma) of dark and light ground areas of known brightness in the aerial photograph. The highly-reflective area serves as a reference for total transmission, while the density of the area of low reflectance provides information on the effects of haze. The haze adds non-image-forming radiance to the

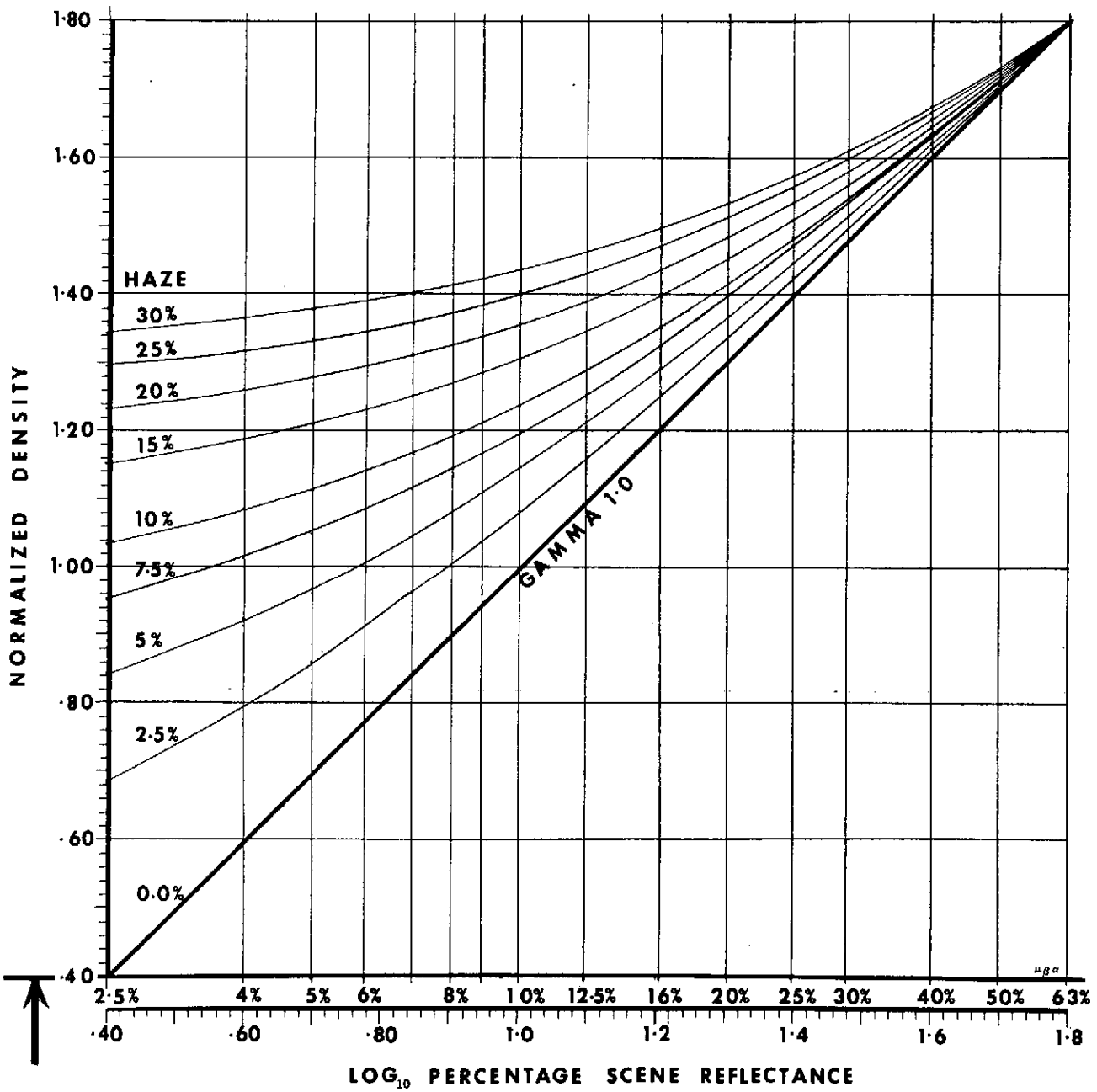

Figure 3-6 Effects of different percentages of haze light on distorting linear reproduction of scene brightnesses. Normalized density values are for the photographic negative. Light attenuation is taken to be 37% for one air mass, with average aerosol content, in the green spectral region.(5)

scene in the object space viewed by the sensor. In a scene where, for example, one subject has 5% reflectance and another 50%, their brightness ratio is 1:10; if a 10% haze factor is added to each they appear to have 15% and 60% reflectance and the brightness ratio is reduced to 1:4. ERTS images are reproduced at $\gamma 1.0$, which reproduces the scene as the sensor saw it, including the scene contrast as reduced by the haze.

The nature, mixture and concentration of aerosols determines the magnitude of light-scattering in each of the spectral bands sensed by ERTS-1, resulting in a different haze factor for each. Invariably, RBV-1 and MSS-4 have the highest haze factors.

3.6 In the ERTS-1 images at 1:1,000,000 scale, large light and dark natural formations whose reflectance properties are known, or can be estimated with some accuracy can be used as references for calculating a probable haze factor. Heavy, white cloud and calm ocean surface can provide such reference areas for evaluating ERTS image densities in terms of probable haze percentages. In doing this, several assumptions are made:

(a) That images of heavy cloud represent 100% sensor response in any ERTS spectral band, and would be at zero density in a normalized positive image.

(b) That the image of calm, clean, deep water will have the highest density in the normalized MSS-7 positive image, because of almost complete infrared absorption by water and minimal haze effects.

(c) That the images to be analyzed are within the gamma and density tolerances specified by NASA/GSFC.

With regard to (c), the specified ERTS-1 image density range is within 0.40 to 2.40 $\pm$0.12, at gamma 1.0 $\pm$0.1. In normalization, where 100% sensor response is at 0.0 D and zero response at 2.0 D, densities in a gamma 1.0 reproduction are represented by the straight line in Figure 3-7. However, at sensor response of less than 20% of full scale, the gamma[2a] of the image scene is less than 1.0, as shown by the curved line formed by joining the decreased density points theoretically resulting from the decreasing gammas at sensor response less than 20%. In interpreting

% Max Sensor Output	Reference (2a) Gradient (Gamma)	Normalized γ 1.0 Film D	Effective Film Density
2.0	0.75	1.70	1.27
3.2	0.80	1.50	1.20
5.0	0.85	1.30	1.10
8.0	0.90	1.10	0.99
12.7	0.95	0.95	0.90
20 Plus	1.00	0.70	0.70

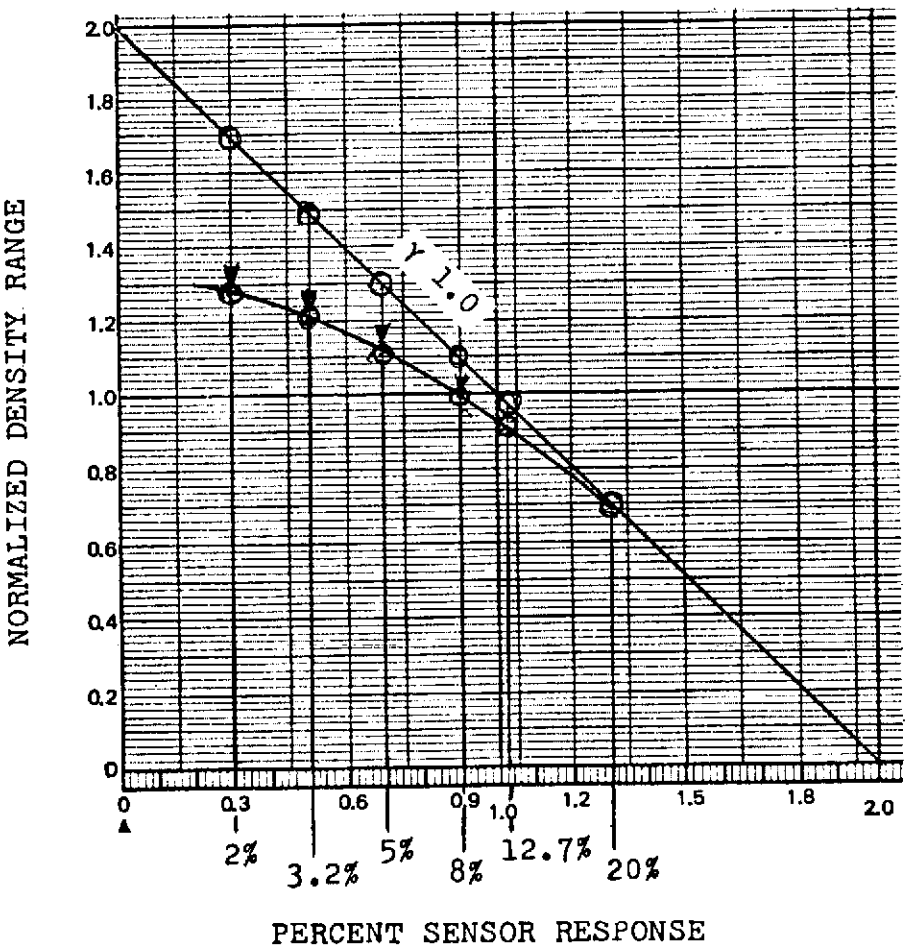

Figure 3-7 γ1.0 line represents linear sensor output plotted against positive image density, where 100% response is 0.0 D and 0% is 2.0 D. Sensor recording gradient (gamma) is less than γ1.0 between 2% and 20%, resulting in decreased densities and contrast in the darker image areas, as shown by the curved line. Effective density is found by multiplying the theoretical γ1.0 density by the actual local gamma, viz 1.70 D x γ0.75 = 1.27 D. Average gamma between 4%-10% is 0.60.

Figure 3-7, it should be noted that a line tangent to the curve, between the points where 4% and 10% response occurs, has a gamma of about 0.60. This is where radiance levels generally associated with blue and green water color information may be recorded in most cases. A decrease from $\gamma 1.0$ in this region of sensor response further decreases the contrast of an ocean scene which already may be affected adversely by haze.

3.7 Deriving Correction Factors by Density Normalization. A number of image areas were selected and measured as density references. Those chosen are noted in Figure 3-2, the two key areas being a heavy cloud (C2) and a deep ocean region (02). In selecting the ocean reference, the MSS-7 infrared image was examined to choose an area of maximum density in the deep water, where it will be seen readily whether or not reflections of sunlight from a disturbed surface or other flaws are present. Shallow water and sand banks, either dry or having not more than a few feet of water served as secondary references. The main reference densities were used as follows:

3.8 Haze Factor. Cloud and water densities were measured in three MSS bands and two RBV bands. (The latter include radiometric correction mask densities.)

Positive Images:	MSS-7	MSS-5	RBV-2	MSS-4	RBV-1
Deep Water:	1.92	1.43	1.45	1.23	1.42
Cloud:	0.58	0.49	0.53	0.50	0.89
Water D Less Cloud:	1.34	0.94	0.92	0.73	0.53

The deep water densities for each band are plotted on graphs of the kind illustrated in Figure 3-7, as shown in Figures 3-8 through 3-12, where the cloud density has been taken as 100% sensor response, or zero density. Referring the densities to the sensor response/equivalent scene reflectance on the abscissa gives this:

Figure 3-8 This and Figures 3-9 through 3-12 illustrate a method of estimating the atmospheric haze factor in each ERTS-1 spectral band. It is based on comparing the densities of light and dark objects in the scene, whose relative orders of reflectance can be approximated with some confidence, and where the sensitometric reproduction characteristics of the image are known within close tolerances. White cloud is taken as 100% sensor response, equivalent to 100% scene reflectance. In the infrared MSS-7 band, deep, clear, calm water is assumed to have 0% reflectance recorded with a minimum of atmospheric haze effects. The density scale of subjects in the scene is normalized by subtracting cloud density, 0.0 D in the positive image being 100% equivalent scene reflectance. In this figure, the deep water surface shows less than 1% reflectance, while the sand area recorded through very shallow water shows 3%.

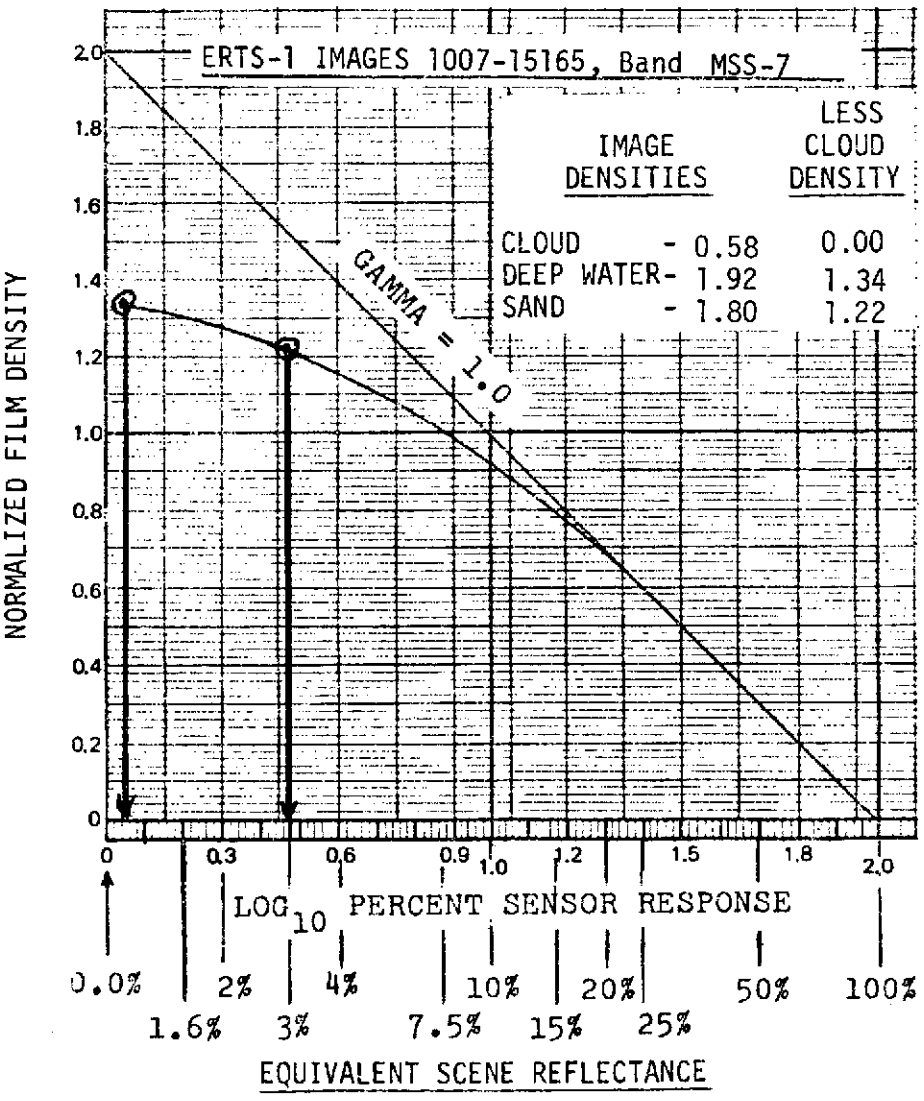

Figure 3-8 ERTS-1 MSS-7 Image.

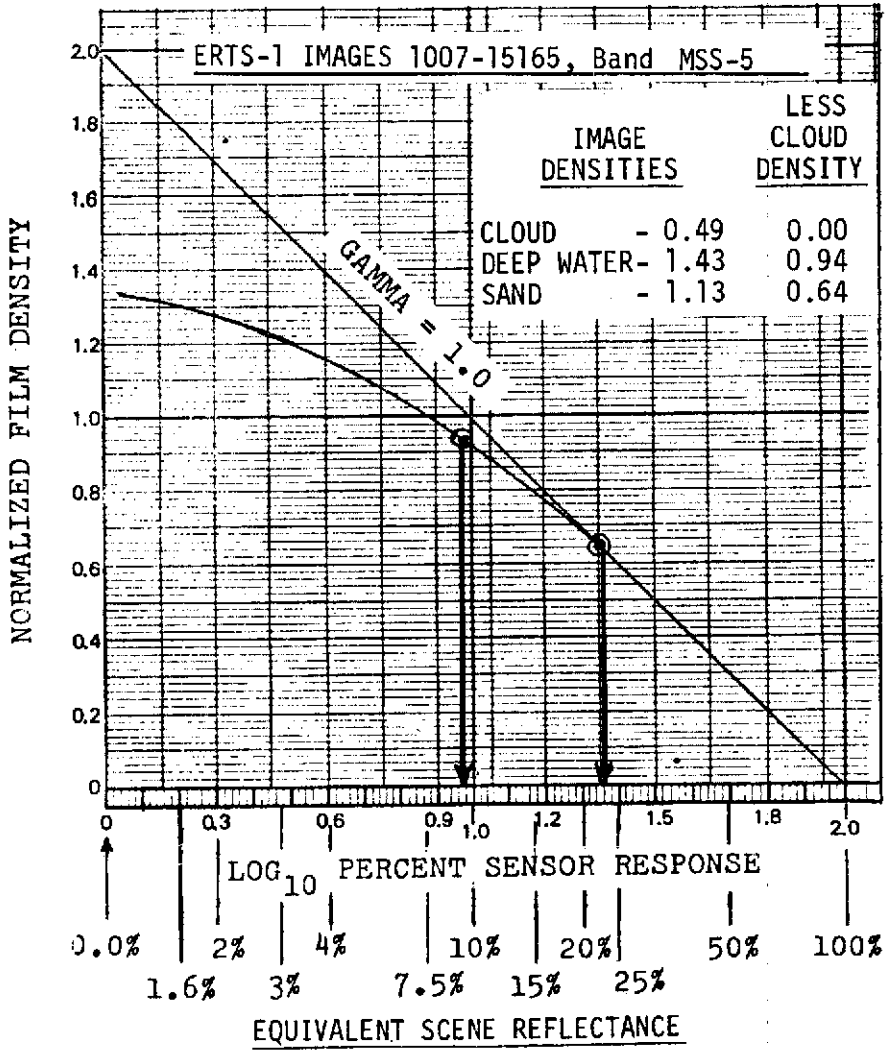

Figure 3-9 ERTS-1 MSS-5 Image.

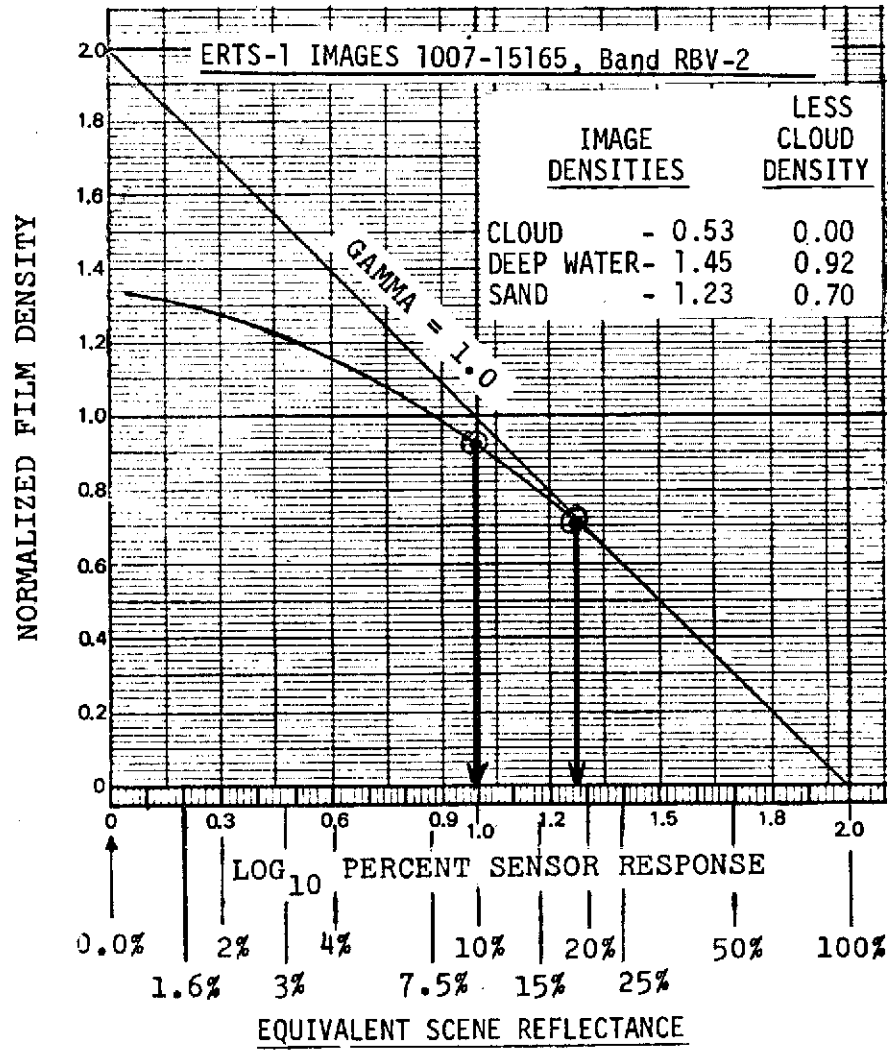

Figure 3-10 ERTS-1 RBV-2 Image.

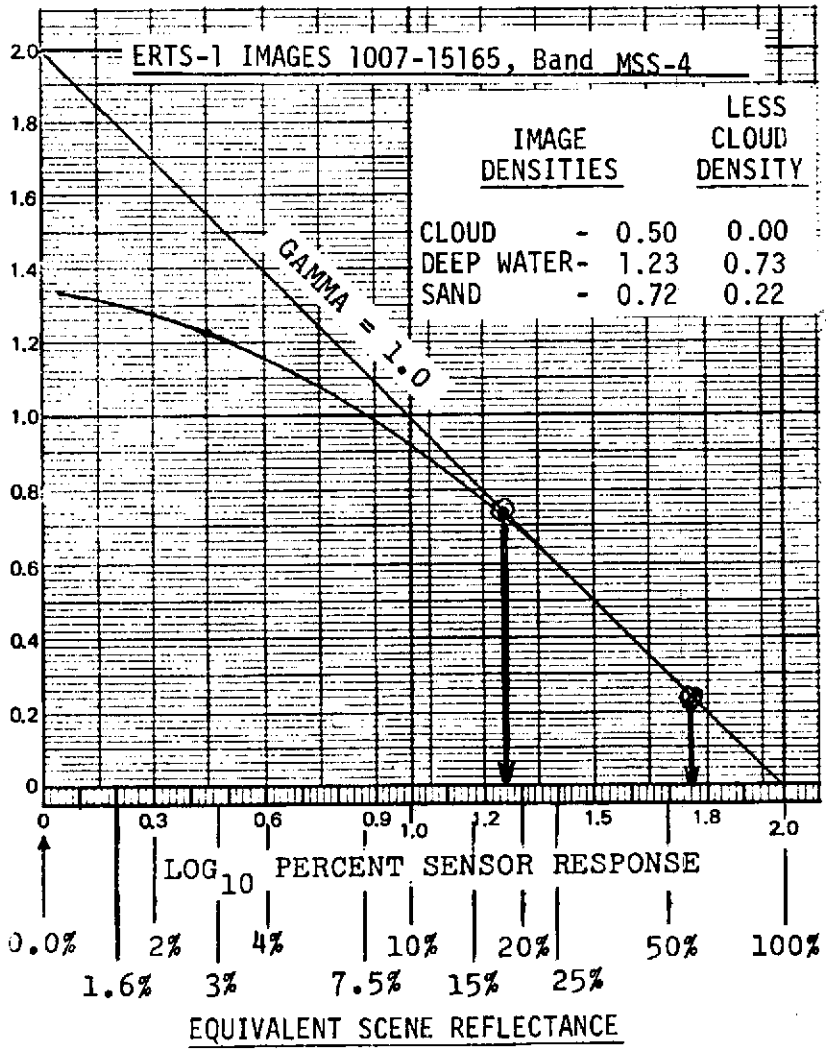

Figure 3-11 ERTS-1 MSS-4 Image.

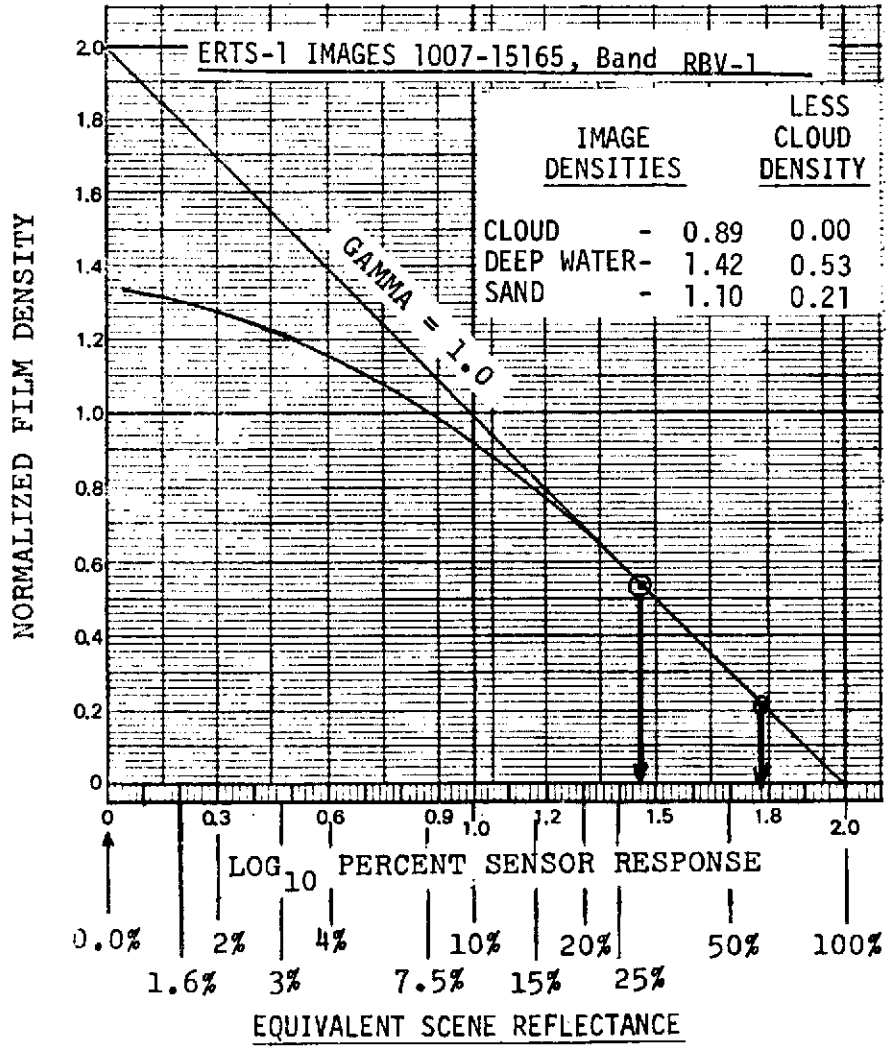

Figure 3-12 ERTS-1 RBV-1 Image.

	MSS-7	MSS-5	RBV-2	MSS-4	RBV-1
Deep Water Percent Reflectance/Sensor Response	<1%	≈10%	10%	18%	29%

From the known reflectance and color characteristics of the deep water, it is inferred that the percent apparent reflectance of infrared band MSS-7 is in the right order.

Of the 10% in the MSS-5 red band, about 7% hazelight is present over and above the 2% or 3% light from the surface; RBV-2 senses in the same spectral region and has a similar haze factor, which will be assumed as 7.5%. The green MSS-4 includes 2%-3% surface, and an equivalent amount of upwelling green light. The RBV-1 similar spectral band includes the same, plus a 465-490 nm region in the deep water contributing blue upwelling light, as well as an increase in the haze factor. The average apparent reflectance of the same deep water region in MSS-4 and RBV-1 is 23%. Within the limitations of this way of density normalization, a haze factor of 15% was adopted for the RBV-1 and MSS-4 images.

As Figures 3-10 through 3-12 show, all normalized image reference densities in RBV-2, MSS-4 and RBV-1 fall on the $\gamma 1.0$ part of the curve, and corrections for sensor response were not required in this case.

3.9 Haze Correction Gamma Factors. The haze curves shown in Figure 3-6 are used to find gamma correction factors required to restore the contrast of the scene to that which it would have had in the absence of haze. RBV-1 and MSS-4 have the same order of haze, 15%, while RBV-2 has a haze factor of about 7.5%. The pertinent haze curves are reproduced in Figure 3-13. Lines are drawn on the average curves between 4% and 10% scene reflectance/sensor response, where deep blue water and green water color radiances would be recorded. The angles the tangent lines form show scene gamma of the RBV-1/MSS-4 images to be reduced by haze from $\gamma 1.0$ to $\gamma 0.19$, and the RBV-2 to $\gamma 0.42$. 100% scene contrast has been reduced by haze about 80% in the one case and 60% in the other.

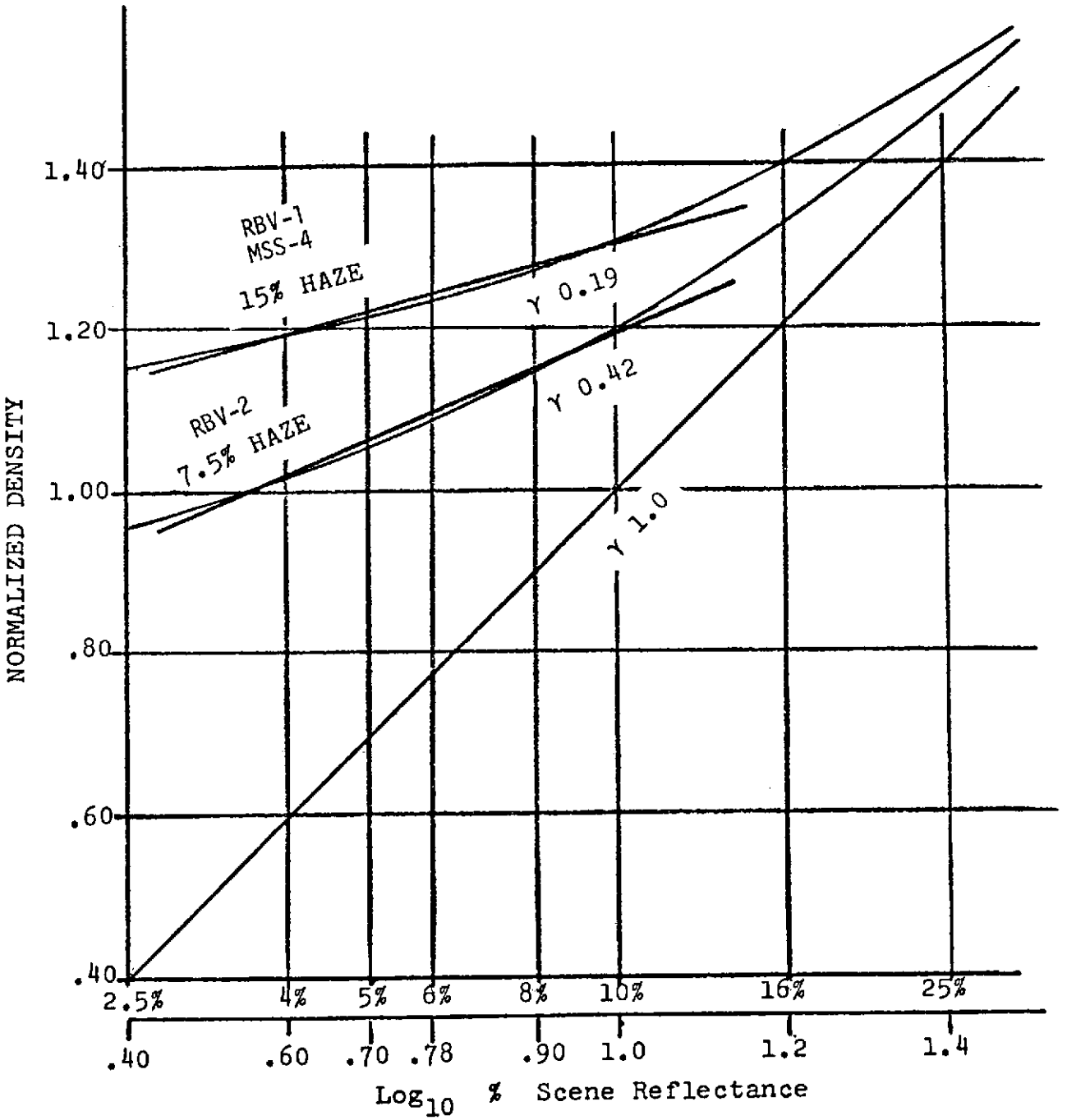

Figure 3-13 Effect of 15% and 7.5% estimated haze factors in reducing 4%-10% scene reflectances from linear $\gamma 1.0$ reproduction to $\gamma 0.19$ and $\gamma 0.42$ for the ERTS-1 RBV-1/MSS-4, and RBV-2 images, respectively.

The images can be reproduced at higher gammas to raise scene contrast (scene gammas) closer to true values, and in a more correct contrast relationship to each other. Reproduction gammas (γ_R) necessary to do this are:

RBV-1 and MSS-4 $\quad \frac{\gamma 1.0}{\gamma 0.19} = \gamma_R\ 5.26$

RBV-2 $\quad \frac{\gamma 1.0}{\gamma 0.42} = \gamma_R\ 2.38$

3.10 Using Gamma Correction Factors. The working images to be used in masking could be corrected in gamma in the first stage of reproduction, as exemplified in the image tone reproduction cycles in Figure 3-14. This was done. As the water and cloud reference densities had to be reproduced on the straight line response of the reproduction films, a high initial density was necessary. Also, the high gamma factor increased the image density range. For example, in the original RBV-2 image, the density range between cloud and deep water was 0.92 (Figure 3-10); at $\gamma 2.38$ this became a range of 2.19 D. In MSS-4 (Figure 3-11) an original range of 0.73 became 3.84 D. The combined image densities of the positive and negative to be printed could exceed 4.0 (0.01% transmittance) or more, and printing times became excessive. In masking, emulsion surfaces of the registered films are separated by the two film base thicknesses, providing a form of unsharp masking (Appendix B). Exposure necessary to print through the combined high densities tended to create edge effects on less dense detail by a form of halation. Evidence of light-piping in the polyester film bases was also found in a few image areas.

Gammas in the final images to correct scene contrast are γ_R 5.26 for the RBV-1 and MSS-4 images, and γ_R 2.38 for RBV-2. Proportionately these are 2.21:1.0. In the final process diagrammed in Figure 3-1, initial masking gammas of the MSS-4 (C) and RBV-1 (G) images were set at $\gamma 2.21$, while the RBV-2 (B) image was retained at $\gamma 1.0$. Thus the 0.92 reference density range of RBV-2 (B) was maintained while that of MSS-4 (C) was only increased to 1.61 from 0.73, the combined densities not exceeding 2.60.

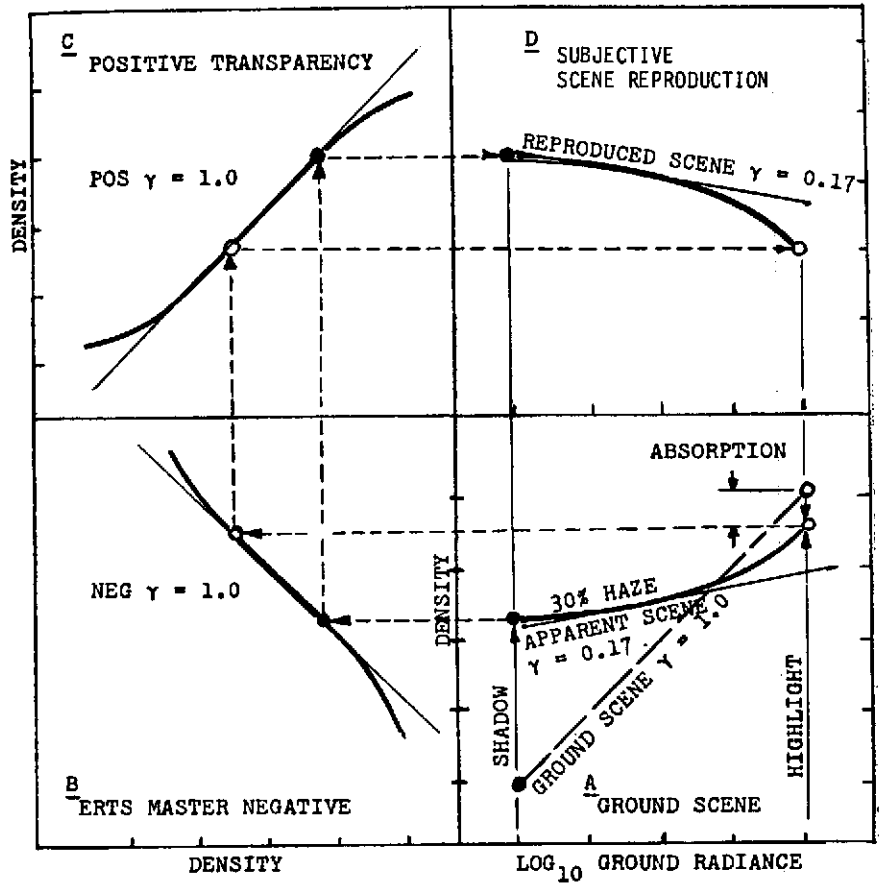

Figure 3-14 Gamma 1.0 scene reproduction cycle, with 30% haze. The negative and positive faithfully reproduce scene radiances as recorded by the sensor through the atmosphere, including the much lower apparent scene gammas in the darker areas of the subject.

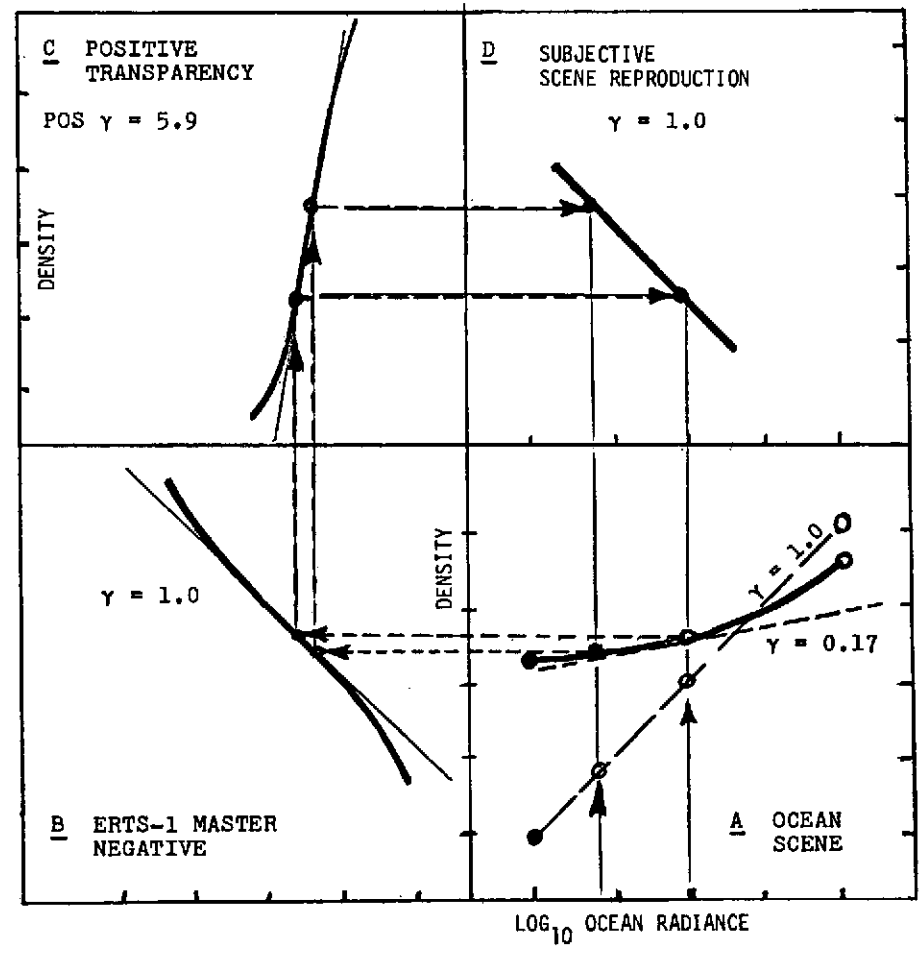

Restoring ocean scene contrast, degraded by haze, to ground level values by reproduction at predetermined gamma - $\left[\frac{1.0}{.17} = \gamma 5.9\right]$
From Reference (1).

3.11 Scene Gamma and Reproduction. In the registered combination of RBV-2 (B) pos $\gamma 1.0$ and MSS-4 (C) neg $\gamma 2.21$, the scene contrast of the latter has been adjusted proportionately to that of the former. The positive image (D) resulting is processed to $\gamma 1.0$, but the ocean scene contrast is reproduced at γ_R 2.21, as noted in Figure 3-1. As (D) is used as a negative mask, it is reprinted to a negative (E), processed to $\gamma 1.0$, but still retaining the required image densities on the straight line of the film curve, with scene contrast remaining γ_R 2.21. The (E) negative registered with RBV-1 (G) γ_R 2.21 matches it in scene gamma, and the product X (or H) when processed at $\gamma 1.0$ retains the scene gamma of the masked combination at γ_R 2.21. The (H) and (G) combination which produces Y (or I) similarly maintains γ_R 2.21, and X and Y are matched.

3.12 Gamma Control. Calibrated step tablets were used in every stage of masking and reproduction for determining that key image densities were on the linear part of the curve. However, the basic reference used for establishing reproduction gamma was the relationship and range of the reference image densities between each stage of reproduction, since the objective was to reproduce the image densities, rather than the step tablet, at predetermined gammas. The form of unsharp masking employed (Appendix B) could alter the effective density printing range of the image plus its mask relative to that of the step tablet. The latter was always in direct contact with the printing material, whereas the image being printed was separated from its mask by the thickness of the two film bases.

3.13 Image Reference Densities. Originally a number of deep and shallow water, cloud and sand areas were used as reference densities. These are identified in Figure 3-2. Experience showed that one deep ocean area (O2) one cloud (C2) and one sand area (B) were sufficient for repeatible sensitometric control. The density difference between the cloud and the deep water represented the extreme density range of significant image information.

3.14 Exposure Control. The reference image densities were also used for exposure control, to ensure their reproduction on the linear part of the reproduction film response curve at each stage.

4.0 SUMMARY OF RESULTS, AND CONCLUCIONS

4.1 Final Density/Gamma Relationships. Figures 4-1 (B) and 4-1 (C) are positive reproductions of the registered sections of negatives X and Y, compared with the original RBV-1 image, Figure 4-1 (A). Contrast has been adjusted for half-tone reproduction. X theoretically represents the 465-490 nm region removed from the RBV-1 record, and Y the 490-580 nm remainder. Density differences between significant parts of the scene, in the γ_R 2.21 negatives are:

	Neg X	ΔD	Neg Y	ΔD
Deep Ocean (02)	1.44		0.64	
		>0.02		>0.66
Bimini Shallows (B)	1.46		1.30	
		>0.16		>0.26
Cloud (C2)	1.62		1.56	

4.2 As noted in Paras 3-10 and 3-11, the gamma required to correct for haze effects in the deep ocean part of the scene was estimated to be γ_R 5.26. This will result in too high a contrast in the more highly reflective parts of the scene, where atmospheric effects have less relative influence. However, the density differences in the low to mid-range of reflectance shown above between the deep water, 02, and the very shallow area B, multiplied by 2.38 (γ_R 2.21 X 2.38 = γ_R 5.26) gives the order of spectral difference between the two:

	Neg X, 465-490 nm	Neg Y, 490-580 nm
ΔD, 02/B	0.05	1.57

4.3 Qualitative Interpretation. Quantitative analysis of this set of images in the absence of ground truth is not possible, but qualitative interpretation shows that the objective of separating the original RBV-1 image into two spectral bands has been successful for the deep water, as can be seen in Figure 4-1 (B) and (C). The ocean in the vicinity of 02 is much lighter in X than in Y, since the 465-490 nm blue region predominates over the green 490-580 nm image.

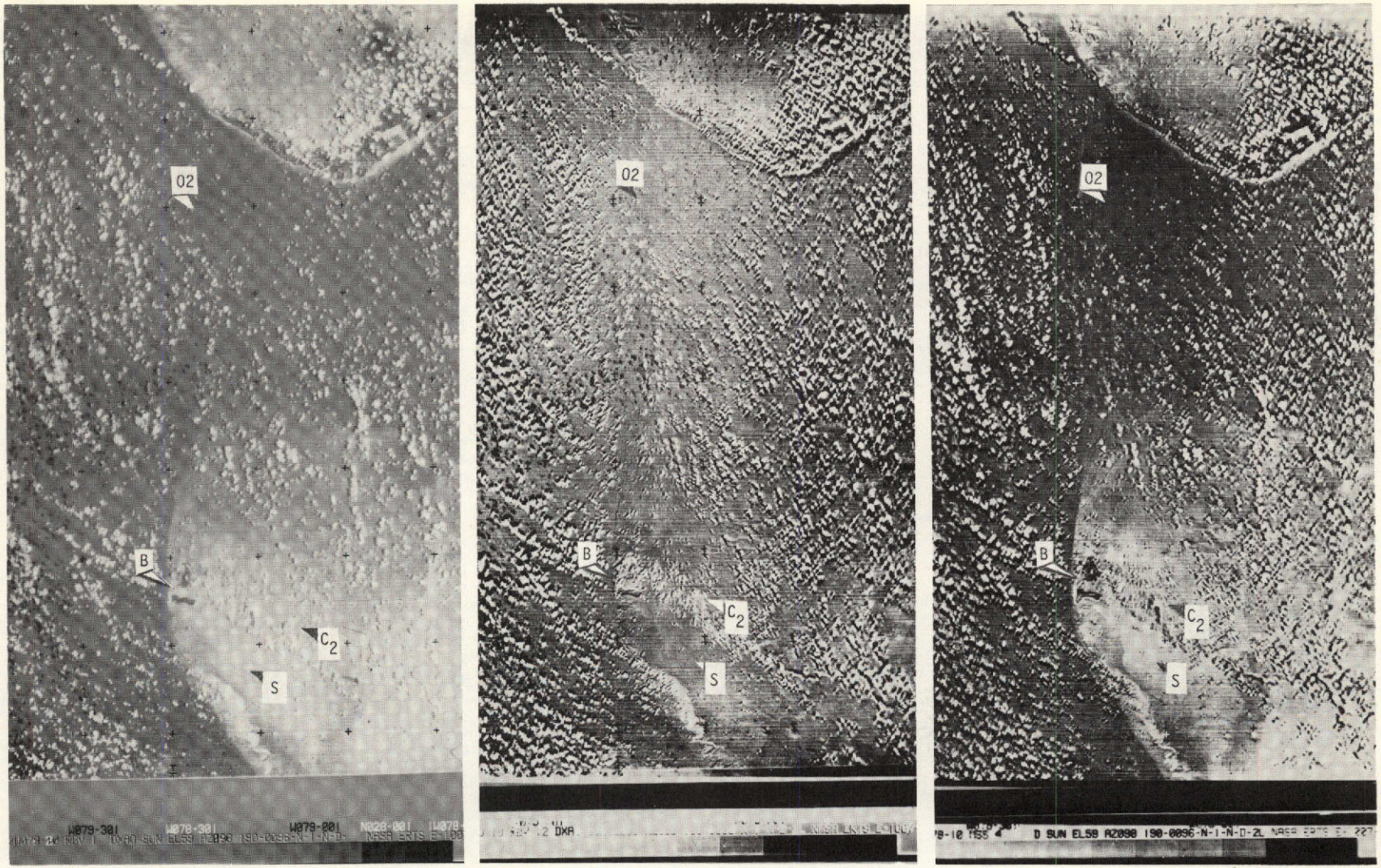

A. RBV-1 Original 465 nm - 580 nm spectral band.

B. Print from negative X, 465 nm - 490 nm.

C. Print from negative Y, 490 nm - 580 nm.

Figure 4-1 Positive prints of the registered sections negatives X and Y, compared with the same section in the original RBV-1 image, from which they were extracted.

The sand flat B, between North & South Bimini Islands is noted on the chart as dry at low tide. This area has a higher density in red MSS-5 than in the green MSS-4 band (Figures 3-9 and 3-11) rather than the equal reflectivity in these two regions shown for typical Bahamian sand in Figure 2-3. It is inferred that the sand flat is submerged in perhaps 0.5 meter of water. In negatives X and Y, however, the area B has about the same order of density as would be expected in the blue and green spectral regions, in shallow water.

Relative to cloud reference C2, area B has lesser density difference in X than in Y, ΔD 0.16 vs. 0.26; whereas the two should be about the same. Some overmasking in the brighter parts of the scene may be occurring, accounting for the noticeable density difference between X and Y in the region S, where water is nominally 1.5 to 2.5 meters deep. The densities should be similar.

Overmasking of the lighter, more reflective parts of the scene was expected, as the original recording of the scene is non-linear. The haze factors and gamma correction data shown in Figure 3-13 were for a 4%-10% deep water scene reflectance range, whereas in the shallow areas the reflectance range is probably 10% to 20%. Under the same haze conditions the gamma factor of the higher reflective range for RBV-1/MSS-4 is about γ0.42 for RBV-2. To properly mask the shallow areas, the proportional gamma relationships shown in Figure 3-11 would be modified from γ_R 2.21 to γ_R 1.40, following the procedures in Paras 3.9 and 3.10.

4.4 Comparison with Color Photography. Visual comparison with Gemini and Apollo images of this area shows the distinctive cyan hue in the shallow water and deep blue in the deep water. NASA/MSC image GT VII S65-63825 (Dec. 5, 1965) is typical and includes the Bahamas, Andros, New Providence and Berry Islands. The RC-8 image NASA/MSC #147-1, 0195, scale 1:120,000 shows similar color effects. The blue and green color densities of these duplicate images cannot be compared directly with the X and Y negatives extracted from the ERTS-1 RBV-1 image, since the peak blue response in the color film is near 450 nm or lower, and sensitivity in the 470-500 nm region is depressed to separate the blue and green records. Also, haze

is not taken into account. Nevertheless, the raw density readings and their percentages of transmittance on the S0118 positive duplicate RC-8 image 147-1, 0195 show the trend in blue and green water color ratios:

	Blue D	Green D
Deep Water	0.77 (17%)	1.29 (5%)
Shallow Water	0.49 (32%)	0.82 (15%)
Area B	0.31 (49%)	0.45 (35%)

In the deep water, the green contributes one third of the upwelling light, but in the shallow water almost one-half, to give the appearance of blue-green.

4.5 Conclusions. This experiment attempted to remove from a 115 nm spectral passband, image densities representing at the most a narrow 25 nm region, where tolerances for input image characteristics could not be established exactly; and by graphical estimations of atmospheric effects and the water color spectrum based on theory. The ERTS-1 images worked with, particularly the RBV images, are among the earliest products of the system, and are not necessarily representative of later improvements in accuracy of scale matching. In this case, the scale mis-match between the three images has restricted the masked area to a narrow band, about 60 by 100 km, greatly reducing the total area which can be used. It is expected that substantial improvements in scale matching, as well as radiometric correction and reproduction sensitometry of the bulk-processed ERTS-B images will simplify the practical application of this technique of water color assessment.

Quantitative applications of the masking technique depend on accurate sensitometric information on the input imagery, and a sufficiently extensive testing of procedures against ground truth data on atmospheric conditions and water color spectrometry.

A major part of the uncertainties would be resolved if the gray scale printed on ERTS images was converted to the form commonly used in photographic sensitometry, with transmittance increments nominally $\sqrt{2}$. This would enable the gamma and form of the ERTS reproduction film curve

to be measured; deviations from norm to be found; establish more accurately the relationship of image densities to the spectral radiation recorded by the sensor. The gray scale would follow the image through each stage of processing to provide quantitative summation of the image characteristics of each generation. The present gray scale does not permit this; in fact none measured by this experimenter has been found to follow the 1/14 systematic scale of values specified.

4.6 It should not be overlooked that where broader spectral bands are concerned, positive results can be derived more directly by masking techniques, and have direct application in the analysis of subjects such as agriculture, hydrology, forestry, geology and urban studies. A negative MSS-5 masking a positive MSS-7 would, for example, generate a new image in which hydrological features were discriminated. This simple form of interactive image processing has potential for greatly broadening the user base by solving or clarifying many everyday remote sensing problems, directly connected with the timely reduction of large amounts of imagery into forms immediately useful to regional governmental and commercial organizations concerned with monitoring and managing Earth's resources.

Appendix A

CHARACTERISTICS OF IMAGE SET UTILIZED

A-1 Cumulative U. S. Standard Catalog No. U-9, Vol. 1; Observation ID Listing, May 31, 1973, Goddard Space Flight Center, provides the following information on the image set used in this experiment:

Observation ID:	1007-15165
Date Acquired:	30 Jul. 1972, Orbit 96
Principal Point:	26.07° N, 79.11° W
Sun:	59.9° Elevation, 98.3° Azimuth
Cloud Cover:	50%
Image Quality:	G, all RBV and MSS bands

A-2 Several film printings of the image set were examined, as positives, 240 mm (9.5-inch), and positive and negative 70 mm. One set of third generation 270 mm positives was selected for best correlation of GSFC gray scale steps between the RBV and MSS images. Density readings for the sensor bands concerned are shown in Table A-1.

The RBV sets agree with each other in the order of density difference between steps, as do the MSS images, but ΔD's between highest densities differ. However, when the measured densities of the deep water areas in the positive images are related to the GSFC gray scale steps of equivalent density, it is found that the ΔD's between the gray scale steps agree closely; as do the densities of shallower water areas.

	RBV-1	RBV-2		MSS-4
Deep Ocean	1.05	1.00		1.23
Shallow Water	0.71	0.71		0.71
GSFC Steps	**ΔD**	**ΔD**	**GSFC Steps**	**ΔD**
4-5	0.20	0.19	3-4	0.21
5-6	0.18	0.13	4-5	0.15
6-7	0.13	0.12	5-6	0.10

Table A-1

NASA/GSFC GRAY SCALE DENSITY READINGS

Step	RBV-1	(ΔD)	RBV-2	(ΔD)	MSS-4	(ΔD)	MSS-5	(ΔD)	MSS-7	(ΔD)
1	2.32		2.30		2.29		2.30		2.32	
		.32		.29		.52		.53		.52
2	2.00		2.01		1.77		1.77		1.80	
		.53		.55		.52		.52		.54
3	1.47		1.47		1.25		1.25		1.26	
		.29		.31		.21		.23		.22
4	1.18		1.15		1.04		1.02		1.04	
		.20		.19		.15		.12		.14
5	0.98		0.96		0.89		0.90		0.90	
		.18		.13		.10		.10		.11
6	0.80		0.83		0.79		0.80		0.79	
		.13		.12		.09		.10		.09
7	0.73		0.71		0.70		0.70		0.70	
8	(Steps 8 and above have insignificant ΔD deviations.)									

All readings include base/fog density. The RBV densities above were read before addition of the radiometric correction masks. It was concluded that the RBV and MSS image densities of the water area are sufficiently linear to each other. All image density readings were re-measured several times by two readers. Control step tablets were measured at least twice. Deviations among the readings were not in excess of $\pm$0.02 D. Figure 3-2 identifies image reference density areas used for exposure and reproduction control.

A-3 A difference in lateral scale (E-W) was found between the RBV and MSS images. Image registration adequate for masking was possible along the N-S axis, and included both deep and shallow water. Image density primary references were selected in the area of best registration to avoid spurious readings.

A-4 Prints of the RBV-1 and -2 images made with their radiometric correction masks contain cloud image artifacts in the western third of the images. These occur in an area of mis-registration between the RBV and MSS images used, and lie outside the part of the composite imagery investigated.

Appendix B

EQUIPMENT, FILMS, AND PROCEDURES

B-1 Printing. All films were printed in an Afga-Gevaert Duplex vacuum printer, exposed to a Colight Model T ceiling source 1.5 meters distant. This unit has remotely selectable filters. Illumination in a 30 cm (12 inch) circle in the printing area was constant within 2%.

B-2 Registration and Masking. Radiometric masks were hand registered and taped on the RBV-1 and -2 images, which were then registration-punched to match the MSS-4 image. All subsequent generations were registration-punched in an Aldiss-Berkey punch, and pinned during printing. A template border mask, also with registration holes, was used in printing and for locating the position of the control step tablet during each reproduction step. The tablet was always placed emulsion-to-emulsion with the print material during the first generation.

In combining the mask in registration with the image to be masked, the latter was placed emulsion to the print material emulsion; the mask emulsion was upward with the two clear film bases face-to-face. This produced a form of unsharp masking and reduced the effects of any mis-registration.

B-3 Processing. All films were tray-processed by hand, in stainless steel trays immersed in a water bath. Electronic timers were used for exposure control and process timing. Developer temperature was monitored with an EK Process Control Thermometer to $\pm$0.3° C at the selected temperature, normally 20° C (68° F). Films were dried in a Goodkin dryer.

B-4 Calibrated Tablet and Sensitometric Control. The same Eastman Kodak calibrated tablet was printed on the reproduction film during each generation for monitoring exposures and processing gammas. However, as explained in Paras 3.12 and 3.13 reference densities selected from key image areas formed primary controls.

B-5 Densitometry. A Macbeth Quantalog TD-102 Densitometer with a 2 mm aperture was used for all density reading. The small image size of the cloud and other reference areas necessitated a 2 mm rather than the 3 mm aperture recommended. The densitometer was checked frequently against the EK calibrated step tablet, and against its internal reference density before each set of readings.

B-6 Films. All reproduction films were 28 X 35.6 cm (11 X 14 inches), the ERTS-1 images being printed in an area about 20 cm (8 inches) square within the central part to avoid border effects in processing.

Several film types were used, processed in different developers and when necessary, at higher temperatures than 20° C (68° F), to obtain linearity at pre-determined gammas in the reproduction density ranges required. On occasion blue, green or red Wratten filters 47B, 61 and 29 were used to filter the exposing source as an aid in straightening the toe of the response curve of some of the films.

The following Kodak emulsions were tested:

Kodalith Ortho, Type 3, 2556
Contrast Process Pan, 4155
Separation Negative Film, Type 1, 4131
Separation Negative Film, Type 2, 4133
Fine Grain Positive, 7302
Commercial Film, 4127
Gravure Positive Film, 4135
Ektapan Film, 4162

With the exception of Kodalith Ortho, Type 3, 0.004-inch Estar Base, all others are 0.007-inch Estar base.

B-7 Developers. The Kodak developers noted below were used at various times with some or all of the films listed. A fresh lot of developer was used for each film processed to ensure consistency. Families of curves were run as required for selecting film developer/temperature/time parameters.

Kodalith Liquid
D-11
D-16
D-19
DK-50
D-76

B-8 Optimum Film/Developer Combinations. The best combinations for linear reproduction at predetermined gammas and low minimum densities were found to be:

$>\gamma 2.0$	- Contrast Process Pan 4155 - D-19
$\gamma 1.5 - \gamma 2.0$	- Separation Negative Film, Type 2, 4133 - DK-50 (Exposure with Wratten 61 filter)
$\gamma 1.0 - \gamma 1.5$	- Gravure Positive, 4135, DK-50
$\approx\gamma 1.0$	- Separation Negative Film, Type 1, 4131 - DK-50 Commercial Film, 4127 - DK-50, D-19

REFERENCES

1. D. S. Ross, Experiments in Oceanographic Aerospace Photography, II-Image Acquisition and Enhancement Techniques, Final Report TR-28-2-73, 28 Feb 73, U. S. Naval Oceanographic Office Contract N62306-71-C-0045.

2. Earth Resources Technology Satellite, Data Users Handbook, Document Number 71SD4249, Goddard Space Flight Center:

   (a) Section H
   (b) Section F.

3. N. G. Jerlov, Optical Oceanography, Elsevier Oceanography Series 5, Elsevier Publishing Co., 1968.

4. J. L. Tupper and C. N. Nelson, The Effect of Atmospheric Haze in Aerial Photography Treated as a Problem in Tone Reproduction, Photographic Engineering, Vol. 6, No. 2, 1955, pp 116-126.

5. D. S. Ross, Atmospheric Effects in Multispectral Photographs, Photogrammetric Engineering, Vol. XXXIX, No. 4, pp 377-384.

6. G. C. Brock, The Physical Aspects of Aerial Photography, Dover Publications, 1967, pp 206, 207.